

## Characteristic Ultrastructural Findings in Metabolic and Storage Diseases

Tokuhiro Ishihara,<sup>1</sup> Mutsuo Takahashi,<sup>2</sup> Toshikazu Gondo,<sup>1</sup> Hiroo Kawano,<sup>1</sup> Yoshinobu Hoshii,<sup>1</sup> Suguru Tamura,<sup>1</sup> Yoshimi Yamashita,<sup>3</sup> Tadaaki Yokota,<sup>4</sup> Toshiaki Kamei,<sup>5</sup> Mayumi Koga,<sup>6</sup> and Fumiya Uchino<sup>7</sup>

<sup>1</sup>First Department of Pathology, <sup>2</sup>Department of Clinical Laboratory Science, <sup>6</sup>Department of Pediatrics, Yamaguchi University School of Medicine, Ube, Yamaguchi 755, Japan

<sup>3</sup>Tokuyama Central Hospital, <sup>4</sup>Kokura Memorial Hospital, <sup>5</sup>Yamaguchi Central Hospital,

<sup>7</sup>Yamato Hospital.

(Received July 15, revised September 6 1994)

**Abstract** Electron microscopic observations performed with immunoelectron microscopy and specific cytochemical stainings play an important role in the diagnosis of diseases affecting carbohydrate, lipid, protein, and mineral metabolism. The characteristic ultrastructural changes in affected cells of metabolic diseases are summarized as follows: (1) many glycogen granules in glycogenosis type I; (2) many glycogen granules in glycogenosis type III; (3) glycogenosomes in glycogenosis type II; (4) curvilinear tubular structures in Farber's disease; (5) myelin-like figures in Niemann-Pick's disease, and in splenic macrophages with idiopathic thrombocytopenic purpura; (6) tubular structures in hemolytic anemia resulting from overproduction of adenosine deaminase; (7) zebra bodies or membranous cytoplasmic bodies in Fabry's disease; (8) vacuoles containing granular and flocculent materials in Hurler's syndrome; (9) vacuoles in sialidosis; (10) vacuoles containing granular, flocculent and myelin-like figures in I-cell disease; (11) membrane-like structures in glycogenosis type IV; (12) membrane-like structures showing a positive reaction with Thiery stains for demonstrating carbohydrate materials in Lafora's disease; (13) nonbranching fibrils, measuring 7-15 nm in width, in the extracellular space and rarely in a few cells from systemic amyloidosis and localized amyloidosis (using immunoelectron microscopy with antibodies to AA, A $\lambda$ , A $\kappa$ ,  $\beta$ 2-microglobulin, and  $\beta$ /A4, we have been able to identify amyloid fibrils in various kinds of amyloidosis); (14) vacuolar inclusions with limiting membrane varying in diameter from 200-300  $\mu$ m to several  $\mu$ m in polyvinyl pyrrolidone thesaurosis; and (15) aurosomes in patients with Felty's syndrome who have received gold sodium thiomalate.

**Key words:** Glycogenosis, Mucopolysaccharidosis, Mucolipidosis, Sphingolipidosis, Amyloidosis, Lafora's disease, Ultrastructure, Metabolic disease

### Introduction

A large number of metabolic diseases, including those affecting carbohydrate, lipid, and protein metabolism, have more or less characteristic ultrastructural cellular changes.

The classification used is that of Dustin et al. (Table 1)<sup>1)</sup>. The figures presented in this article were taken from our personal collection.

Table 1. Metabolic and Storage Diseases

- I. Abnormal Quantities of Normal Metabolites
  - 1) Glycogenesis type I, III, VIII
  - 2) High-density lipoprotein deficiency (Tanger disease)
- II. Abnormal Quantities and Abnormal Location of Normal Metabolites
  - 1) Glycogenesis type II
  - 2) Wolman disease
  - 3) Cholesterol ester storage disease
  - 4) Lipofuscin, ceroid and ceroid-lipofuscinoses
  - 5) Iron (hemosiderosis, hemosiderosis)
  - 6) Copper (Wilson disease)
  - 7) Cystinosis
- III. Accumulation of Intermediary Metabolites
  - 1) Ceramidosis (Farber disease)
  - 2) a) Sphingomyelinosis (Niemann-Pick disease)  
b) Niemann-Pick-like cell in ITP
  - 3) a) Glucosylceramidosis (Gaucher disease)  
b) Gaucher-like cell in thalassemia and hemolytic anemia
  - 4) Galactosylceramidosis (Krabbe disease)
  - 5) Metachromatic leukodystrophy (Sulfatidosis)
  - 6) Ceramide trihexosidosis (Fabry disease)
  - 7) Gangliosidosis
  - 8) Mucopolysaccharidosis (Hurler, Hunter, Sunfilippo A, B diseases)
  - 9) Mucopolidosis (Sialidosis, I-cell disease)
- IV. Accumulation of Abnormal Metabolites
  - 1) Glycogenesis type IV
  - 2) Lafora disease
    - a) Basophilic degeneration of the myocardium
    - b) Corpora amylacea
  - 3) Amyloidosis
- V. Accumulation of Exogenous Materials
  - 1) Polyvinyl pyrrolidone (PVP) thesaurosis
  - 2) Hydroxyethyl starch (HES) thesaurosis
  - 3) Thorotrast thesaurosis
  - 4) Gold thesaurosis

(Modification of Dustin's Classification<sup>1)</sup>)

## Materials and Methods

The observations described below are based on studies of the following tissues:

1. liver obtained at biopsy from a 37-year-old woman with glycogenesis type I,
2. liver and striated muscle obtained at biopsy from a 27-year-old man with glycogenesis type III,
3. striated muscle obtained at biopsy from a 2-year-old boy with glycogenesis type II,
4. skin obtained from excisional biopsy, and skin, liver and small intestine obtained at autopsy from a 2-year-old boy with Farber's disease<sup>2)</sup>,
5. liver and spleen from a 6-year-old girl with Niemann-Pick's disease (C type),
6. spleen obtained at operation from 15 patients aged 5 to 51 (mean 27.8) with idiopathic thrombocytopenic purpura (ITP)<sup>3-5)</sup>,
7. spleen obtained at operation from an 11-year-old boy with hemolytic anemia resulting from overproduction of adenosine deaminase<sup>6)</sup> and commercialized sphingolipids (ceramide with  $\alpha$ -hydroxy fatty acids, ceramide with nonhydroxy fatty acids, glucocerebroside, sphingomyelin) injected subcutaneously to adult normal ICR mice<sup>6)</sup>,
8. heart obtained at operation and kidney,

- liver, spleen, and heart obtained at autopsy from a 47-year-old man with Fabry's disease,
9. peripheral blood from a 5-year-old boy with Hurler's syndrome,
  10. kidney, spleen, liver, heart, and placental tissue obtained at autopsy from a 3-month-old girl and a 20-week sibling fetus with sialidosis,
  11. heart, spleen, liver, kidney, and placental tissue obtained at autopsy from a 1-year-old boy and two fetuses (20 and 19 weeks siblings) with I-cell disease<sup>7)</sup>,
  12. liver obtained at biopsy from a 3-month-old girl with glycogenosis type IV and liver at biopsy, and liver, heart, and spleen at autopsy from an elder brother (6-month-old boy) with glycogenosis type IV<sup>8,9)</sup>,
  13. brain, myocardium and liver obtained at autopsy from a 20-year-old woman and a 26-year-old man (sibling) with Lafora's disease<sup>10)</sup>, and brains obtained at autopsy from aged dogs<sup>11)</sup>,
  14. liver, heart and intestine obtained at biopsy from four patients with AA amyloidosis, four patients with AL amyloidosis, and ligaments obtained at operation from two patients with A $\beta$ 2M amyloidosis,
  15. intestine obtained at biopsy from a 62-year-old man with localized A $\lambda$  amyloidosis<sup>12)</sup>,
  16. urinary bladder obtained at biopsy from three patients with localized A $\lambda$  amyloidosis,
  17. brains obtained at operation from five patients with amyloid angiopathy and at autopsy from aged dogs,
  18. lymph node from a 32-year-old woman intravenously injected with a small amount of polyvinyl pyrrolidone (PVP) after hysterectomy five years earlier<sup>13)</sup>,
  19. spleens obtained at operation from a 52-year-old man and a 60-year-old woman with Felty's syndrome<sup>5)</sup>. They had received a total of 4.895 and 55 mg of gold sodium thiomalate, respectively.

For transmission electron microscopy, small pieces of tissues were fixed in 2.1% glutaraldehyde with and/or without postfixation in 1% osmium tetroxide, dehydrated through a graded series of ethanol solutions,

transferred to propylene oxide, and embedded in Epon 812.

The periodic acid-thiosemicarbazide-silver proteinate method of Thiery<sup>14)</sup> was used for the electron microscope demonstration of periodate-reactive vicinal glycols. For this method the grids were placed in 1% aqueous periodic acid for 30-45 minutes; washed with water; treated with either 1% thiosemicarbazide or 0.2% thiocarbohydrazin in 10% acetic acid for one hour; washed with several changes of 10%, 5% and 1% acetic acid; rinsed in water; placed in 1% aqueous silver proteinate for 30 minutes in the dark and washed with water.

For immunoelectron microscopy, plastic-embedded blocks were used with the following immunoperoxidase staining method: ultrathin sections were pretreated for one hour with a saturated aqueous solution of sodium metaperiodate, according to the method of Bendayan and Zollinger.<sup>15)</sup> After washing in 0.01 M phosphate-buffered saline (PBS), pH 7.4, the tissues were labeled with colloidal gold as follows: (a) 1% bovine serum albumin in PBS for 30 minutes; (b) antibodies (anti-Lafora body, anti-AA, anti-A $\lambda$ , anti-AK, anti- $\beta$ 2 microglobulin, anti- $\beta$ /A4) for four hours; (c) protein A-colloidal gold complex for one hour. All incubations were performed at room temperature. After washing in PBS, rinsing in distilled water, and drying, the sections were stained with uranyl acetate and lead citrate, and observed with Hitachi HS-8, H-300, H-800, and H-7000 electron microscopes.

## Results and Discussion

### I. Deposition of Abnormal Quantities of Normal Metabolites

#### *Glycogenosis Type I (von Gierke's Disease)*<sup>16,17)</sup>

Glycogenosis type I is caused by a deficiency of glucose-6-phosphatase. Patients with the disorder are characterized by massive hepatomegaly, failure to thrive, and severe hypoglycemia, particularly during infancy. Inheritance is autosomal recessive. The diagnosis is established by demonstrating increased contents of glycogen with normal structure in a liver biopsy and absent

glucose-6-phosphatase activity.

#### Light Microscope Findings.

Hepatocytes were enlarged and had abundant pale cytoplasm. The cytoplasm was strongly stained with periodic acid-Schiff (PAS). PAS-positive inclusions were digested by diastase. In the Glisson sheath, connective tissue was increased and pseudolobuli were formed.

#### Ultrastructural Findings.

In glycogenosis type I, excessive quantities of a normal metabolite are stored in a normal location and with a normal ultrastructural aspect.

We found many glycogen granules located in the cytoplasm and nucleus (Fig. 1). The particles of  $\beta$  glycogen granules were spherical in shape and measured from 20 to 40 nm in diameter. Hepatocytes also contained lipid droplets.

#### *Glycogenosis Type III (Cori's Disease)*<sup>16,18)</sup>

Glycogenosis type III, known as debrancher (amylo-1, 6-glucosidase) deficiency, is an autosomal-recessive disorder similar to glycogenosis type I, although clinically more mild. Hepatomegaly may be noted in infancy and the consequences of hypoglycemia may occur.

#### Light Microscope Findings.

Hepatocytes had clear cytoplasm and excessive deposition of glycogen showing diastase-sensitive, PAS-positive materials (Fig. 2). Histochemically, both glucose-6-phosphatase and acid phosphatase activities were present in the hepatocytes as they were in the control cases. Amylo-1, 6-glucosidase activity was, however, absent in the hepatocytes, although present in the control livers.

In semi-thin sections, metachromatic materials showing the compacted and altered glycogen were seen in the cytoplasm and nucleus of hepatocytes.

#### Ultrastructural Findings.

In glycogenosis type III, a normal metabolite was stored in excessive quantities, in a normal location and with a normal ultrastructural aspect. Markedly, hepatocytes and striated muscle cells showed numerous rosettes of  $\alpha$  glycogen granules located in the cytoplasm and nucleus (Figs. 3, 4, 5). The particles of  $\beta$  glycogen granules were spheri-

cal in shape and measured from 20 to 40 nm in diameter. The cell organelles were not affected. No glycogen granules accumulated in the lysosomes as the glycogenosome, and  $\alpha$ -glucosidase were normal.

The ultrastructural aspect did not differ qualitatively from that in secondary glycogen overload, as seen in diabetes mellitus. The absence of lysosomal changes is of diagnostic value. In the hepatocytes of a patient with glycogenosis type III, we found intramitochondrial and intranuclear glycogen deposits in addition to a large amount of accumulations in the main cytoplasmic compartment.

#### II. Abnormal Quantities and Abnormal Location of Normal Metabolites

##### *Glycogenosis Type II (Pompe's Disease)*<sup>16,18)</sup>

Pompe's disease, recognized as the first lysosomal storage disease, is classified clinically into infantile, juvenile, and adult types. Deficiency of lysosomal acid  $\alpha$ -glucosidase accounts for a massive accumulation of glycogen virtually in all tissues. It has been proposed that neutral  $\alpha$ -glucosidase deficiency, most marked in the infantile and least in the adult form, explains the differing clinical expressions. The disease, in all forms, is autosomal recessive.

Diagnosis may also be made on the basis of tissue biopsy. Typical lysosomal-bound glycogen aggregates are found within various cells in the skin and conjunctival biopsies.

#### Light Microscope Findings.

The striated muscle cells had pale or vacuolar cytoplasm. The pale cytoplasm contained PAS-positive materials. PAS-positive inclusions were digested by diastase.

In semi-thin sections, metachromatic materials showing the compacted and altered glycogens were sometimes seen in the cytoplasm of striated muscle cells.

#### Ultrastructural Findings.

A large number of glycogen particles were located within lysosomes, called glycogenosomes or glycogenolysosomes, in striated muscle cells (Figs. 6, 7). The glycogen granules were monogranular with a single particle having a diameter of approximately 25 nm. A moderate number of glycogen particles were also freely dispersed in the

cytoplasm of the myocytes, where they existed in the morphologically normal monoparticulate or  $\beta$ -form. Most of the cytoplasmic glycogen was in the rosette form.

Cellular change in Pompe's disease was presumed to arise from the rupture of fragile lysosomes and, indeed, low mitochondrial enzyme activity is probably a marker of such organelle damage.

### III. Accumulation of Intermediary Metabolites

#### *Ceramidosis (Farber's Disease)*<sup>2)</sup>

Farber's lipogranulomatosis is a rare progressive disorder of lipid metabolism resulting from a deficiency of lysosomal acid ceramidase and characterized by hoarseness, painful and swollen joints, periarticular and subcutaneous nodules, pulmonary infiltrations, and the accumulation of lipids in the cytoplasm of neurons and certain other cells. Accumulation of ceramide, deficiency of lysosomal acid ceramidase, or both have been demonstrated in affected patients.

#### Light Microscope Findings.

Subcutaneous nodules on both the lip and perianal regions had a similar histologic appearance, including elongation of the rete ridges, proliferation of the collagen fibers and capillaries, and scattered spindle- or oval-shaped cells. These cells had an enlarged cytoplasm which was positive for colloidal iron, alcian blue, and PAS prior to diastase digestion, and showed occasional metachromasia with toluidine blue staining. The tinctures of various lipid stainings were as follows: orange red in Sudan III, orange in Sudan IV, black in Sudan black B, and blue in Nile blue sulfate. These results indicate that affected cells contain acid or neutral polysaccharides and lipid. Typical foamy cells were rarely seen, and the histochemical findings were similar to those of spindle- or oval-shaped cells, except that foamy cells were stained more weakly for lipid stainings than were spindle- or oval-shaped ones. Such granulomas were present in the periarticular region, larynx, and pericardium.

#### Ultrastructural Findings.

The spindle- or oval-shaped cells in the subcutaneous nodules—which were considered to be fibroblasts and macrophages, respective—

lyhad an enlarged cytoplasm and membrane-bound intracytoplasmic inclusions containing flocculent, granular, or fibrillar materials, with a few curvilinear tubular structures. These structures were termed "Farber bodies" and consisted of two electron-dense lines separated by clear space. The average diameter of the tubules was 15 nm. Macrophages and endothelial cells in the spleen also had intracytoplasmic inclusions containing fibrillar materials.

Farber bodies were induced in animals by injection of ceramides and related sphingolipids. Farber bodies were noted in the cytoplasm of cutaneous macrophages in mice that received a single dose of ceramide with  $\alpha$ -hydroxy fatty acids, ceramide with nonhydroxy fatty acids, glucocerebroside, and sphingomyelin<sup>19)</sup>.

#### *Sphingomyelinosis (Niemann-Pick's Disease)*<sup>20)</sup>

Sphingomyelin lipidoses are characterized by accumulation of sphingomyelin (ceramide phosphoryl choline) in certain organs and tissues of affected individuals.

Sphingomyelinase deficiency is classified into three clinical forms as types A, B, and C. All three types are of autosomal-recessive inheritance. A sphingomyelin lipidosis occurring in families of Nova Scotian ancestry, similar to type C but lacking evidence of sphingomyelinase deficiency, has been called type D Niemann-Pick's disease. Adult patients found incidentally to have a moderate sphingomyelin excess in one or more organs, but without evidence of familial involvement, have been considered to have "type E" Niemann-Pick's disease. Reports of sphingomyelinase deficiency in some of these patients require further confirmation.

#### Light Microscope Findings.

Multiple-vacuolated foamy cells were typical of Niemann-Pick's disease. A large number of foamy cells were noted in the liver and spleen. In the liver, hepatocytes also had a large number of vacuoles. The foamy cell had a pale or clear cytoplasm, often vacuolated in appearance, with tinges of yellow or brown reflecting variable lipofuscin content.

#### Ultrastructural Findings.

A large number of myelin-like materials were

demonstrated in the cytoplasm of Kupffer cells, hepatocytes (Fig. 8) and macrophages in the spleen. There were myelin-like inclusions, pleomorphic bodies with dense and lucent zones, and dense granules, presumably lipofuscin.

#### *Niemann-Pick-like Cells in Idiopathic Thrombocytopenic Purpura*<sup>3-5)</sup>

Since Landing et al.<sup>21)</sup> and Saltzstein<sup>22)</sup> first reported the occurrence of lipid-containing histiocytes in the spleens of patients with idiopathic thrombocytopenic purpura (ITP), there have been many reports about the foamy cells in ITP<sup>3-5,23,24)</sup>.

#### Light Microscope Findings.

The spleens contained variable numbers of foamy cells in the medullary cords, occasionally forming small nests. They had pale cytoplasm with irregular granular and poorly defined, foamy vacuolation. They had a few PAS-positive materials, and some of them stained black with Sudan black B. Occasional foamy cells contained variable amounts of immunoreactive materials to anti-human platelet antibody.

#### Ultrastructural Findings.

Variable numbers of macrophages usually contained numerous myelin-like materials varying in size and shape (Fig. 9). The foamy cells demonstrated on light microscopy were thought to be those containing numerous myelin-like materials on electron microscopy. Platelet phagocytosis by cordal macrophages was frequently encountered, and morphologic transition between engulfed platelets and myelin-like materials was readily demonstrated.

#### *Gaucher-like Cells*<sup>5)</sup>

Foamy histiocytes that resemble true Gaucher cells in many respects have been called "Gaucher-like cells" or "Gaucher-type cells." Since the original description by Sen Gupta et al. in 1960<sup>25)</sup>, Gaucher-like cells in the bone marrow, spleen, and occasionally in the liver have been reported in different hematologic disorders, most frequency in chronic granulocytic leukemia (CGL) and thalassemia.

#### Light Microscope Findings.

A large number of foamy cells were noted in

the red pulp and marginal zone of the spleen. Most of them formed small nests in the cordal spaces and occasionally in the sinuses. The foamy cells, measuring on average 20–50  $\mu\text{m}$  in size, were polygonal, round, or oval in shape, and the cytoplasm was often pale and vacuolated. The nucleus was vesicular and eccentrically located. These foamy cells were stained reddish purple with PAS after diastase digestion, blue with alcian blue, and pale yellow with van Gieson's stain. There were a few granular materials in the cytoplasm stained with Sudan III and Sudan black B. Some cells revealed a sea-blue appearance with May-Giemsa stain. These foamy cells contained strong acid phosphatase and  $\beta$ -glucuronidase activity. Histochemical demonstration of acid phosphatase activity was the most valuable special stain.

#### Ultrastructural Findings.

Large macrophages containing numerous inclusions and a few lysosomes were demonstrated in the red pulp. The foamy cells in the semi-thin sections stained with toluidine blue were estimated to correspond with these macrophages. The inclusions varied in diameter from 0.5  $\mu\text{m}$  to several microns. They were ovoid, polygonal, or irregular in shape and mostly surrounded by a single membrane. These cytoplasmic inclusions were composed of variable amounts of tubule-like structures that were measured approximately 7–9 nm in width. Tubule-like structures were usually straight and did not branch (Fig. 10). Acid phosphatase activity was demonstrated in the cytoplasmic inclusions (Fig. 11), although the activity varied among the cells. Some inclusions contained a few dense bodies, which were intermingled with the tubule-like structures. Some macrophages with the tubule-like cytoplasmic inclusions revealed erythrophagocytosis. Although various stages of intracellular degradation of engulfed erythrocytes were noted, transitions between the phagocytosed erythrocytes and tubule-like inclusions were not discernible.

#### *Ceramide trihexosidosis (Fabry's Disease)*<sup>26-28)</sup>

Angiokeratoma corporis diffusum universale or Fabry's disease was described in 1898 in England by Anderson and in Germany by Fabry. The disease is a hereditary systemic

glycolipidosis of sex-linked recessive type caused by a congenital deficiency of ceramide-trihexosidase. A detailed ultrastructural description of the affected cells present in Fabry's disease was reported by Henry et al. on the kidney biopsy specimen<sup>26)</sup>.  
Light Microscope Findings.

In ordinary histologic sections, various kinds of vacuoles were observed in muscle cells, endothelial cells, pericytes, and macrophages. In osmium tetroxide-fixed sections, the materials showed dark brown. In frozen sections, they were sudanophilic, PAS-positive, and strongly birefringent.

In semi-thin sections, various kinds of inclusions were demonstrated in the cardiomyocytes.

#### Ultrastructural Findings.

The deposits were diverse in fine structural appearances. In cardiomyocytes and endothelial cells these deposits occupied the central, perinuclear areas, displacing the contractile elements toward the periphery (Figs. 12, 13). Some were spherical, rod-shaped and finger-print-like, while others were fleecelike, striped, and even amorphous. The basic components were, however, lamellar myelin-like structures with a periodicity of about 6 nm (Fig. 14).

By Thiery staining, these lamellae displayed a positive reaction with the periodate-thiosemicarbazide-silver proteinate and periodate-thiosemicarbazide-osmium tetroxide methods demonstrating carbohydrate materials ultrastructurally.

#### *Mucopolysaccharidosis*<sup>29)</sup>

The mucopolysaccharidoses comprise a group of diseases characterized by an intracellular storage and a urinary excretion of partially degraded mucopolysaccharides (glycosaminoglycans). The main clinical features are dysmorphism (gargoylism) arising from more or less severe skeletal changes (dysostosis multiplex), mental retardation of variable intensity, and signs of visceral involvement. The increased mucopolysacchariduria (most often dermatan- and heparan-sulfate, alone or in combination) allows researchers to distinguish clearly these syndromes from other clinically related

metabolic disorders, such as mucopolidoses, and oligosaccharidoses.

#### *Hurler's Syndrome*<sup>30)</sup>

Hurler's syndrome is the prototype for all mucopolysaccharide storage diseases. It is a severe, progressive disorder leading to death, usually before the age of ten years. Patients with Hurler's syndrome are clinically normal in infancy. Indeed, they may be unusually large in the first year of life, but thereafter they progressively deteriorate, both mentally and physically. The same enzyme,  $\alpha$ -L-iduronidase, is deficient in Hurler's and Scheie's syndromes.

#### Light Microscope Findings.

Various kinds of vacuoles were noted in the cytoplasm of lymphocytes in peripheral blood. The small part of vacuoles were stained with colloidal iron.

#### Ultrastructural Findings.

In the lymphocytes of peripheral blood, the cytoplasm contained a large number of inclusions. The inclusions showed large, electron-lucent, membrane-limited vacuoles, believed to be altered lysosomes. Acid phosphatase reaction demonstrated the lysosomal nature of the inclusions.

#### *Mucolipidosis*

##### *Sialidosis*

Mucolipidosis I is the least common type of mucolipidosis. As described by Spranger et al., it is characterized by Hurler-like facies, skeletal dysplasia, cherry red macula, progressive ataxia, myoclonic epilepsy, mental retardation, and death in childhood<sup>31)</sup>. As the primary defect in the disorder, a decrease in the activity of neuraminidase was verified by Killy and Graetz in 1977<sup>32)</sup>. The disease of infantile onset in sialidosis was then classified as sialidosis type II by Loden and O'Brien in 1979<sup>33)</sup>. Sialidosis is a rare genetic condition. Type II sialidosis is characterized by severe psychomotor deficiency, growth retardation, a coarse facies, chondrodystrophy, hepatomegaly, abnormal pigmentation and anemia<sup>34)</sup>. To our knowledge, less than 30 cases of sialidosis have been reported in the literature.

#### Light Microscope Findings.

Various kinds of cells contained cytoplasmic

vacuoles. The vacuoles were stained blue with colloidal iron. They were almost completely digested with sialidase. Some of them reacted positively with anti-wheat germ agglutinin and anti-calf fetuin. Vacuoles stained blue with colloidal iron were demonstrated in the following cells or tissues: macrophages of generalized organs, sinusoidal lining and Kupffer cells, hepatocytes, sinus lining cells (spleen, accessory spleen, adrenal glands, pituitary gland), capillary endothelial cells, epithelial cells of glomerular tuft, proximal tubules, follicular cells in the thyroid gland, islets of Langerhans, sweat glands, sebaceous glands, nerve cells in the central nervous system, peripheral nerves, and syncytiotrophoblasts and Hofbauer cells in placental tissues.

#### Ultrastructural Findings.

The inclusions in various kinds of cells, such as hepatocytes (Fig. 15), epithelial cells in the glomerular tuft (Fig. 16), Kupffer cells, sinusoidal lining cells, and so on, consisted of accumulated vacuoles varying in diameter from 200 to 700 nm. Most of these vacuoles were clearly delineated by a unit membrane containing flocculent materials. In some vacuoles, there were a few dense materials and myelin-like structures. These vacuoles were not stained with Thiery's method.

Peripheral lymphocytes, and syncytiotrophoblasts and Hofbauer cells in placenta also were vacuolated.

Ultrastructural studies of various tissues (conjunctiva, skin, bone marrow, and liver) from affected children demonstrated a generalized storage of fibrillogranular material in lysosomes<sup>34</sup>. Jauniaux et al. emphasized that a storage disorder such as sialic acid storage disease can be accurately diagnosed by electron microscopy on chorionic villous specimens at nine to ten weeks<sup>35</sup>.

#### *I-Cell Disease (Mucopolipidosis II)*<sup>7)</sup>

Inclusion-cell (I-cell) disease is transmitted as an autosomal-recessive disorder characterized by a deficiency of multiple lysosomal hydrolase (N-acetylglucosamine-1-phosphotransferase), which acts in the degradation of lipids and mucopolysaccharides and results in an accumulation of large pleomor-

phic inclusions in a variety of cell types. The inclusion bodies result from or are caused by an accumulation of unhydrolysed materials in the lysosomes.

#### Light Microscope Findings.

Lymphocytes had many vacuoles of various sizes in the cytoplasm. Neutrophils had vacuoles less frequently than did lymphocytes. Syncytiotrophoblasts and Hofbauer cells in the placental tissue had many vacuoles measuring 1-15  $\mu\text{m}$  in diameter, but the cytotrophoblasts did not. Podocytes and endothelial cells in the glomerulus had many vacuoles, whereas mesangial and epithelial cells of the Bowman's capsules and renal tubules had few. The Kupffer cells and the macrophages of the spleen both had a few small vacuoles. Some vacuoles were stained positively with colloidal iron (Fig. 17), PAS, and alcian blue. A small number of vacuoles stained positively with Sudan III and Sudan IV.

#### Ultrastructural Findings.

The intracytoplasmic vacuoles surrounded by a single membrane contained inclusion bodies of various sizes (0.4-5.0  $\mu\text{m}$ ) (Fig. 18). Syncytiotrophoblasts had a large number of intracytoplasmic inclusion bodies (Fig. 19). Inclusion bodies were 1-5  $\mu\text{m}$  in diameter. Inclusion bodies in the Hofbauer cells and fibroblasts were smaller (0.4-0.7  $\mu\text{m}$ ) than those in syncytiotrophoblasts. Most of the inclusion bodies were electron-lucent, but some were electron-dense and contained vesicular, granular, flocculent, or rarely lamellar structures. Other cells, e. g. endothelial cells had smaller vacuoles containing only two or three types of inclusion bodies, such as granular or electron-dense inclusion bodies. Acid phosphatase activity was demonstrated in some vacuoles.

#### IV. Accumulation of Abnormal Metabolites *Glycogenosis Type IV (Andersen's Disease)*<sup>8,9,36,37)</sup>

Glycogen storage disease type IV is an extremely rare disorder caused by a recessively inherited deficiency of  $\alpha$ -1, 4-glucan-6-glycosyl transferase, also known as brancher enzyme. Because this disease is a generalized disorder, at autopsy many tissues, but particularly heart and liver, contain



amylopectin-like inclusions. The disease is often diagnosed by liver biopsy.

#### Light Microscope Findings.

Hepatocytes were enlarged and contained abundant pale basophilic materials strongly stained with PAS (Fig. 20). These PAS-positive inclusions showed various features such as a spherical or polygonal shape, and their central cores were diastase-resistant. The material was immunohistochemically reacted with anti-Lafora body (anti-LAc) antibody<sup>37</sup>.

In the myocardium, a large amount of PAS-positive material was seen in the sarcolemma. The deposits were irregular in shape and bore clefts.

#### Ultrastructural Findings.

Irregularly shaped inclusions were seen in the cytoplasm of hepatocytes (Fig. 21), and were composed of glycogen rosettes, glycogen granules, membrane-like structures varying in width from 5 to 15 nm, fine granules, and crumpled materials. In general, glycogen rosettes and glycogen granules were situated in the peripheral areas of the inclusions. In the central area, large numbers of membrane-like structures were randomly arranged and intermingled with the crumpled materials. No limiting membrane was noted at the periphery of the inclusions.

The central area of the sarcolemma of cardiac muscle contained similar inclusions showing an accumulation of the membrane-like structures ranging in width from 5 to 15 nm. Glycogen granules and membrane-like structures were visualized as aggregates of silver particles by Thiery stain (Fig. 22).

#### *Lafora's Disease*<sup>9,37</sup>

Lafora's disease is a hereditary degenerative disorder characterized by seizure, dementia, and myoclonal attacks. Morphologically, it can be distinguished by the presence of large PAS-positive intraneural inclusions which were first described by Lafora in the central cortex, and are thus known as "Lafora bodies." In addition, abnormal deposits were noted, to a lesser extent, in the liver, heart, striated muscle, and skin.

#### Light Microscope Findings.

Lafora bodies were recognized as various-

sized spheroids which were intensely stained with PAS and colloidal iron. The deposits were irregular in shape and often had clefts. Some parts of the inclusions were strongly PAS positive (Fig. 23), and others were weakly positive.

Basophilic inclusions which were thought to be degenerative products were noted in the cytoplasm of myocardial cells and hepatocytes. The deposits were strongly stained with both PAS and colloidal iron. Furthermore, Lafora bodies and the basophilic inclusions also reacted positively with anti-LAc antibody (Fig. 24)<sup>37</sup>.

#### Ultrastructural Findings.

The large inclusions were often laminated and consisted of basophilic-staining cores surrounded by pale zones of radially oriented membrane-like structures (Figs. 25, 26). Some of them consisted of a dense, homogeneous core and a pale radially striated periphery; others were entirely homogeneous.

The deposits accumulated in the myocardial fibers were not membrane-bound, and contained fine electron-dense particles, fibrillar components and crumpled plates.

By Thiery stain, the membrane-like structures and associated electron-dense clumps in both Lafora's disease (Fig. 27) and glycogenosis type IV were intensely stained. The intensity of the staining was almost identical among Lafora bodies, the inclusions in the myocardium from Lafora's disease, and the inclusions in hepatocytes and myocardium from glycogenosis type IV. Both the fibrils and the amorphous materials were seen as aggregates of silver particles.

In immunoelectron microscopy, the membrane-like structures were specifically labeled by gold particles, indicating a reactivity to the anti-LAc antibody. Under higher magnification it could be seen that the gold particles lay directly upon these structures.

#### *Intraneuronal Polyglucosan Bodies in Brains from Aged Dogs*<sup>10</sup>

There have been a few reports of polyglucosan bodies (PGBs) present in aged animals with Lafora's disease.

#### Light Microscope Findings.

PGBs were observed in the brains of five

aged dogs, mainly in the thalamus, mesencephalon and cerebellum, neural perikarya, and cytoplasmic processes. The inclusions appeared as basophilic round bodies measuring up to 10  $\mu\text{m}$  in diameter and stained with PAS.

Immunohistochemically, the marginal zone of the large inclusions was strongly reactive for the anti-LAc antibody, but the core was only weakly reactive.

#### Ultrastructural Findings.

The inclusions were limited to neural processes with synaptic vesicles. The membrane-like structures ranged in width from 5 to 20 nm. In addition to the fibrillar components, accumulated substances often organized into irregular, crumpled plates.

#### Immunoelectron Microscope Findings.

The inclusions composed of the membrane-like structures were specifically labeled with gold particles, indicating reactivity to the anti-LAc antibody (Fig. 28).

### *Amyloidosis*

The deposition of amyloid results from a pluricausal disturbance of protein metabolism. This substance is characterized by its staining properties and the principal ones are its birefringence and dichroism after Congo red stain and its ultrastructure. Among the fibril proteins established as being the unique and morphologically identical components of all amyloids so far described, proteins related to the following precursor molecules have been found which are the basis of the classification recently proposed<sup>38</sup>: (1) serum amyloid A protein (AA); (2) immunoglobulin light chains (AL),  $\lambda$  chain more frequently than  $\kappa$  chain; (3) immunoglobulin heavy chain (AH); (4) transthyretin (ATTR); (5)  $\beta$ 2-microglobulin ( $A\beta$ 2M); (6) cystatin C (ACys); (7)  $\beta$  protein precursor ( $A\beta$ ); (8) procalcitonin (ACal); (9) scrapie protein (AScr); (10) gelsolin (AGel); (11) atrial natriuretic factor (ANF); and (12) Islet amyloid polypeptide (AIAPP).

#### Light Microscope Findings.

An amorphous, structureless substance was deposited in the interstitium of every organ in various kinds of systemic amyloidosis and of certain organs in localized amyloidosis. The substances showed eosinophilic in

hematoxylin-eosin-stained preparations. The substances exhibited orange-red with Congo red stain and showed birefringence and dichroism under polarized light (Fig. 29).

#### Ultrastructural Findings<sup>39,40</sup>.

Amyloid fibrils of all types have virtually uniform ultrastructural and biophysical characteristics regardless of various chemical compositions of their protein subunits. They were composed of nonbranching, fine fibrils, measuring approximately 7-15 nm in width (Fig. 30). The fibrils were usually arranged in random orientation and occasionally formed bundles.

Amyloid fibrils were seen mainly in the interstitia of the various organs, including liver, spleen, kidney, heart, gastrointestinal tract, thyroid gland, and so on.

Parenchymal cells in each organs, e.g. hepatocytes and cardiomyocytes, had pressure atrophy.

Amyloid fibrils of hemodialysis-associated amyloidosis ( $A\beta$ 2M amyloidosis) were arranged in short curvilinear bundles (Fig. 31)<sup>41</sup>.

Intracytoplasmic amyloid fibrils were noted in several cases, mainly in localized amyloidosis<sup>12,42,43</sup>.

Fusiforms to irregular-shaped inclusions, 0.5 to 1.0  $\mu\text{m}$  wide and 1 to 5  $\mu\text{m}$  long, were noted in the cytoplasm of a plasma cell (Fig. 32). These inclusions were always surrounded by a unit membrane bearing ribosomes on its outer surface, indicating that it was rough endoplasmic reticulum (rER) (Fig. 33). The inclusions comprised tightly packed, regular arrays of fine fibrils cut in both longitudinal and cross-sections. The fibrils within the inclusions were always oriented parallel to the long axis of the inclusions. On cross-section, the distance between the centers of adjacent fibrils was 20 nm. Serial sections of the plasma cell with fibrils in the rER showed no fibrils in other organelles, including the Golgi apparatus and lysosomes.

In the immunoelectron microscopic preparations, the reaction product (gold particles) to anti-human  $A\lambda$  antiserum was always associated with the extracellular amyloid deposits. Numerous gold particles also labeled the fibrils within the rER of the

plasma cell (Fig. 34).

Recently, Takahashi et al. reported immunoelectron microscope findings in shoulder tissue from a patient with A $\kappa$  and A $\beta$ 2M amyloidosis. In the immunoelectron microscope preparations with double stainings, gold particles specifically labeled each A $\kappa$  and A $\beta$ 2M amyloid fibrils in the same section.<sup>44)</sup>

#### V. Accumulation of Exogenous Materials<sup>13)</sup> *Polyvinyl Pyrrolidone Thesauriosis*

As polyvinyl pyrrolidone (PVP) widely used as a plasma expander, markedly deposits in the organs of the reticuloendothelial system, it has not been used as a therapeutic drug in recent years.

##### Light Microscope Findings.

A large number of foreign-body granulomas were detected in the subcapsular region in lymph nodes. Some reticulum cells and multinuclear giant cells contained vacuolar inclusions. The inclusions were stained pale blue with hematoxylin and eosin, orange with Congo red, and blue with caledon blue. Vacuolar inclusions were negative with fat stains.

##### Ultrastructural Findings.

Different types of vacuolar inclusions were seen in the cytoplasm of reticulum cells and giant cells. Vacuolar inclusions surrounded by a limiting membrane were round or oval in shape, and they had different electron density and varied in diameter from 200-300 nm to several  $\mu$ m. Occasionally, they contained many osmiophilic granules (perhaps lipid), tubular crystals (probably calcium), and dense bodies.

#### *Gold Thesauriosis*<sup>5)</sup>

The place of gold salts in the treatment of rheumatoid arthritis was firmly established in a multicenter, controlled trial in 1960. At the cellular and subcellular level, gold is concentrated in the lysosomes of tissue macrophages. Electron microscopy in animals treated with soluble gold salts shows localization of those salts into morphologically distinct lysosomal bodies which Ghadially et al. has termed "aurosomes"<sup>45)</sup>.

##### Light Microscope Findings.

Blackish brown pigments, which were stained with Prussian blue, were noted in foamy cells and macrophages in the spleen. These foamy cells had strong acid phosphatase activity.

##### Ultrastructural findings.

Macrophages contained a large number of myelin-like materials, many dense bodies, and a few vacuoles. The most characteristic finding of these cells was the presence of numerous needle-shaped dense bodies within

the phagolysosomes (Figs. 35, 36). By X-ray microanalysis, it was shown that these dense bodies contained gold (Fig. 36).

#### References

- 1) Dustin, P., Tondeur, M. and Libert, J.: Metabolic and storage diseases. In V Johannesen ed. *Electron Microscopy in Human Medicine*. New York, St Louis, San Francisco, Tokyo, Toront. McGraw-Hill 1978, pp. 149-245
- 2) Koga, M., Ishihara, T., Uchino, F. and Fujiwaki, T.: An autopsy case of Farber's lipogranulomatosis in Japanese boy with gastrointestinal involvement. *Acta Pathol. Jpn.*, 42:42-48, 1992.
- 3) Ishihara, T., Matsumoto, N. and Uchino, F.: Foamy histiocytes in the spleen associated with idiopathic thrombocytopenic purpura. *Acta Pathol. Jpn.*, 24:273-284, 1974.
- 4) Ishihara, T., Akizuki, S., Yamanami, S., Yamashita, Y., Yokota, T., Okuzono, Y., Takahashi, M., Kamei, T., Uchino, F. and Matsumoto, N.: Foamy cells in ITP spleens and in granulomas induced by murine platelets, commercialized phospholipids, and erythrocytes membrane. Histological and ultrastructural studies. *Acta Pathol. Jpn.*, 35:943-958, 1983.
- 5) Ishihara, T., Yamashita, Y., Okuzono, Y., Yokota, T., Takahashi, M., Kamei, T., Uchino, F., Matsumoto, N., Miwa, S., Fujii, H., Kozaki, T.: Three kinds of foamy cells in the spleen: Comparative histochemical and ultrastructural studies. *Ultrastruct. Pathol.*, 8:13-23, 1985.
- 6) Ishihara, T., Akizuki, S., Yokota, T., Takahashi, M., Uchino, F. and Matsumoto, N.: Foamy cells associated with platelet phagocytosis. *Am. J. Pathol.*, 114:104-111, 1984.
- 7) Koga, M., Ishihara, T., Hoshii, Y., Uchino, F., Matsuo, K., Yamashita, Y.: Histochemical and ultrastructural studies of inclusion bodies found in tissues from three siblings with I-cell disease. *Pathol. Int.*, 44:223-229, 1994.
- 8) Ishihara, T., Uchino, F., Adachi, H., Takahashi, M., Watanabe, S., Tsunetoshi, S., Fujii, T. and Ikee, Y.: Type IV glycogenosis -A study of two cases-. *Acta*

- Pathol. Jpn.*, 25:613-633, 1975.
- 9) Ishihara, T., Yokota, T., Yamashita, Y., Takahashi, M., Kawano, H., Uchino, F., Kamei, T., Matsumoto, N., Kusunose, Y. and Yamada, M.: Comparative study of the intracytoplasmic inclusions in Lafora disease and type IV glycogenosis by electron microscopy. *Acta Pathol. Jpn.*, 37: 1591-1601, 1987.
  - 10) Yamanami, S., Ishihara, T., Takahashi, M. and Uchino, F.: Comparative study of intraneural polyglucosan bodies in brains from patients with Lafora disease and aged dogs. *Acta Pathol. Jpn.*, 42:787-792, 1992.
  - 11) Ishihara, T., Gondo, T., Takahashi, M., Uchino, F., Ikeda, S., Allsop, D. and Imai, K.: Immunohistochemical and immunoelectron microscopical characterization of cerebrovascular and senile plaque amyloid in aged dogs' brain. *Brain Res.*, 548:196-205, 1991.
  - 12) Ishihara, T., Takahashi, M., Koga, M., Yokota, T., Yamashita, Y. and Uchino, F.: Amyloid fibril formation in the rough endoplasmic reticulum of plasma cells from a patient with localized A $\lambda$  amyloidosis. *Lab. Invest.*, 64:265-271, 1991.
  - 13) Ishihara, T., Uchino, F., Ohnishi, H. and Kamei, T.: Ultrastructural study of PVP thesaurosis in lymph node. *J. Clin. Elect. Microsc.*, 7:311-312, 1974.
  - 14) Thiery, J.: Mise en evidence des polysaccharides sur coupes en microscopie electronique. *J. Microsc.*, 6:987-1018, 1967.
  - 15) Bendayan, M. and Zollinger, M.: Ultrastructural localization of antigenic sites on osmium-fixed tissues applying the protein A-gold technique. *J. Histochem. Cytochem.*, 31:101-109, 1983.
  - 16) Howell, R. R. and Williams, J. C.: The glycogen storage diseases. In Stanbury, J. B., Wyngaarder, J. B., Fredrickson, D. S., Goldstein, J. L. and Brown, M. S. (eds): *The Metabolic Basis of Inherited Disease*. 5th ed. McGraw-Hill, New York, 1983, pp141-166.
  - 17) McAdams, A. J., Hug, C. and Bove, K. E.: Glycogen storage disease, type I to X. Criteria for morphologic diagnosis. *Human Pathol.*, 5:463-487, 1974.
  - 18) Hug, G., Garancis, J. C., Schubert, W. K. and Kaplan, S.: Glycogen storage disease, types II, III, VIII and IX. A biochemical and electron microscopic analysis. *Am. J. Dis. Child.*, 111:457-474, 1966.
  - 19) Koga, M., Ishihara, T. and Uchino, F.: Farber bodies found in murine phagocytes after injection of ceramids and related sphingolipids. *Virchows Arch. A. [Cell Pathol.]*, 62:297-302, 1992.
  - 20) Brady, R. O.: Sphingomyelin lipidoses: Niemann-Pick disease. In Stanbury, J. B., Wyngaarder, J. B., Fredrickson, D. S., Goldstein, J. L. and Brown, M. S. (eds): *The Metabolic Basis of Inherited Disease*. 5th ed. McGraw-Hill, New York, 1983, pp831-841.
  - 21) Landing, B. H., Strauss, L., Crocker, A. C., Braunstein, H., Henley, W. L., Will, J. R. and Sanders, M.: Thrombocytopenic purpura with histiocytosis of the spleen. *New Eng. J. Med.*, 265:572-577, 1961.
  - 22) Saltzstein, S. L.: Phospholipid accumulation in histiocytes of splenic pulp associated with thrombocytopenic purpura. *Blood* 18:73-88, 1961.
  - 23) Firkin, B. G., Wright, R., Miller, S. and Stokes, E.: Splenic macrophages in thrombocytopenia. *Blood*, 16:1039-1044, 1960.
  - 24) Luk, S. C., Musclow, E. and Simon, G. T.: Platelet phagocytosis in the spleen of patients with idiopathic thrombocytopenic purpura (ITP). *Histopathology*, 4:127-136, 1980.
  - 25) Sen Gupta, P. C., Chatterjee, J. B., Mukherjee, A. M. and Chatlerji, A.: Observations on the foam cells in thalassemia. *Blood*, 16:1039-1044, 1960.
  - 26) Henry, E. W. and Rally, C. R.: The renal lesion in angiokeratoma corporis difusum. *Cand. M. A. J.*, 89:206-213, 1963.
  - 27) Ferrans, V. J., Hibbs, R. G. and Burda, C. D.: The heart in Fabry's disease. A histochemical and electron microscopic study. *Am. J. Cardiol.*, 24:95-110, 1969.
  - 28) Elleder, M., Ledvinova, J., Vosmik, F., Zeman, J., Stejskal, D. and Lageron, A.: An atypical ultrastructural pattern in Fabry's disease: a study on its nature and

- incidence in 7 cases. *Ultrastruct. Pathol.*, 14:467-479, 1990.
- 29) McKusick, V. A. and Neufeld, E. F.: The mucopolysaccharide storage diseases. In Stanbury, J. B., Wyngaarder, J. B., Fredrickson, D. S., Goldstein, J. L. and Brown, M. S. (eds): *The Metabolic Basis of Inherited Disease*. 5th ed. McGraw-Hill, New York, 1983, pp. 751-777.
- 30) Renteria, V. G., Ferrans, V. J. and Roberts, W. C.: The heart in the Hurler syndrome. Gross, histologic and ultrastructural observations in five necropsy cases. *Am. J. Cardiol.*, 38:487-501, 1976.
- 31) Spranger, J., Gehler, J. and Gantz, M.: Mucopolidosis I - A sialidosis. *Am. J. Med. Genet.*, 1:21-29, 1977.
- 32) Killy, T. and Graetz, G.: Isolated acid neuraminidase deficiency: A distinct lysosomal storage disease. *Am. J. Med. Genet.*, 1:31-46, 1977.
- 33) Lowden, J. and O'Brien, J.: Sialidosis: A review of human neuraminidase deficiency. *Am. J. Hum. Genet.*, 31:1-18, 1979.
- 34) Tondeur, M., Libert, J., Vamos, F., Van Hoof, F., Thomas, G. H. and Strecker, G.: Infantile form of sialic acid storage disorder: clinical, ultrastructural and biochemical studies in two siblings. *Eur. J. Pediatr.*, 139:142-147, 1982.
- 35) Jauniaux, E., Vamos, E., Liebert, J., Elkhazen, N., Wilkin, P. and Hustin, J.: Placental electron microscopy and histochemistry in a case of sialic acid storage disorder. *Placenta* 8:433-442, 1987.
- 36) Schroder, J. M., May, R., Shin, Y. S., Sigmund, M. and Nase-Huppmeier, S.: Juvenile hereditary polyglucosan body disease with complete branching enzyme deficiency (type IV glycogenosis). *Acta Neuropathol.*, 85:419-430, 1993.
- 37) Yokota, T., Ishihara, T., Yoshida, H., Takahashi, M., Uchino, F. and Hamanaka, S.: Monoclonal antibody against polyglucosan isolated from the myocardium of a patient with Lafora disease. *J. Neuropathol. Exp. Neurol.*, 47:572-577, 1988.
- 38) Kazatchkine, M. D., Husby, G., Araki, S., Benditt, E. P., Benson, M. D., Cohen, A. S., Frangione, B., Glenner, G. G., Natvig, J. B. and Westermark, P.: Nomenclature of amyloid and amyloidosis. WHO-IUIS Nomenclature sub-committee. *Bull WHO*, 71:105-108, 1993.
- 39) Shirahama, T. and Cohen, A. S.: High-resolution electron microscopic analysis of the amyloid fibril. *J. Cell Biol.*, 33:679-708, 1967.
- 40) Uchino, F.: Pathological study on amyloidosis. Role of reticuloendothelial cells in inducing amyloidosis. *Acta Pathol. Jpn.*, 17:49-82, 1967.
- 41) Floege, J., Brandis, A., Nonnast-Daniel, B., Westhoo-Bleck, M., Tiedow, G., Linke, R. P. and Kock, K. M.: Subcutaneous amyloid-tumor of beta-2-microglobulin origin in a long-term hemodialysis patient. *Nephron*, 53:73-75, 1989.
- 42) Takahashi, M., Yokota, T., Yamashita, Y., Ishihara, T., Uchino, F., Imada, N. and Matsumoto, N.: Unusual inclusions in stromal macrophages in a case of gelatinous drop-like corneal dystrophy. *Am. J. Ophthalmol.*, 99:312-319, 1985.
- 43) Takahashi, M., Yokota, T., Ishihara, T., Uchino, F. and Kamei, T.: Insular amyloid in a case of type III glycogenosis with a special reference to the origin of amyloid fibrils. *Ultrastruct. Pathol.*, 10:235-240, 1986.
- 44) Takahashi, M., Hoshii, Y., Kawano, H., Ishihara, T., Matsushita, T., Sawada, S. and Uchino, F.: A case of systemic amyloidosis with simultaneous AL and A $\beta$ 2M amyloid deposition. An immunohistochemical and immunoelectron microscopic study. (in Japanese) *Trans. Soc. Pathol. Jpn.*, 83:311, 1994.
- 45) Ghadially, F. N., Oryschak, A. F., Mitchell, D. M.: Ultrastructural changes produced in rheumatoid synovial membrane by chrysotherapy. *Ann. Rheum. Dis.*, 35:67-72, 1976.

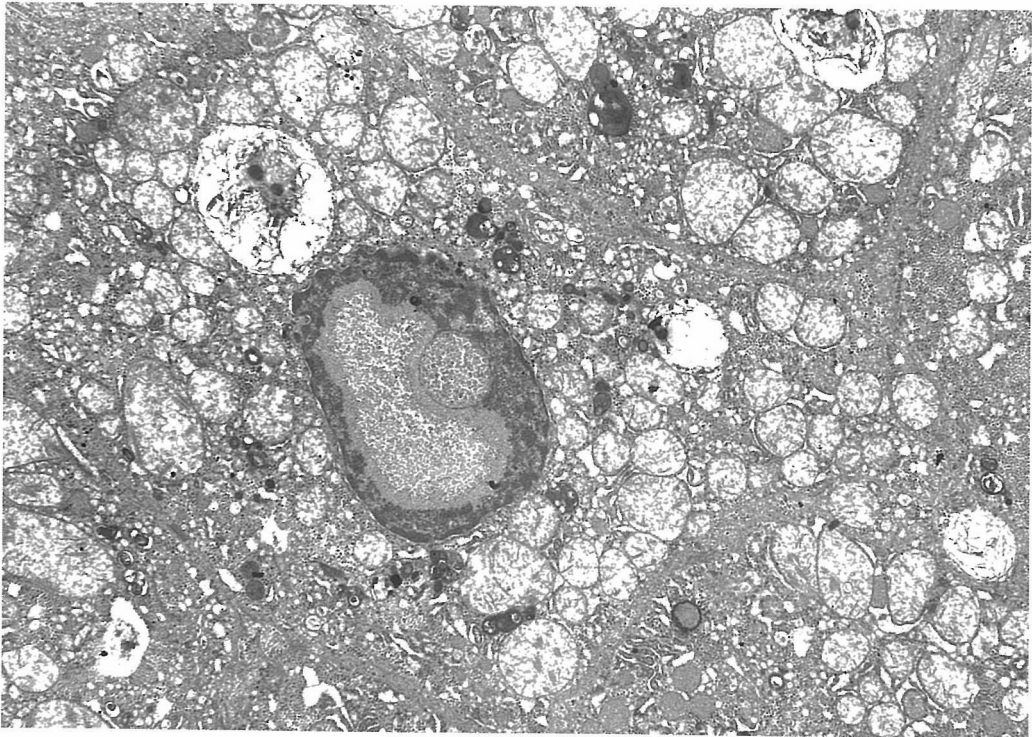


Fig. 1. A large number of glycogen granules are noted in the nucleus of a hepatocyte from a patient with glycogenosis type I.  $\times 3,000$

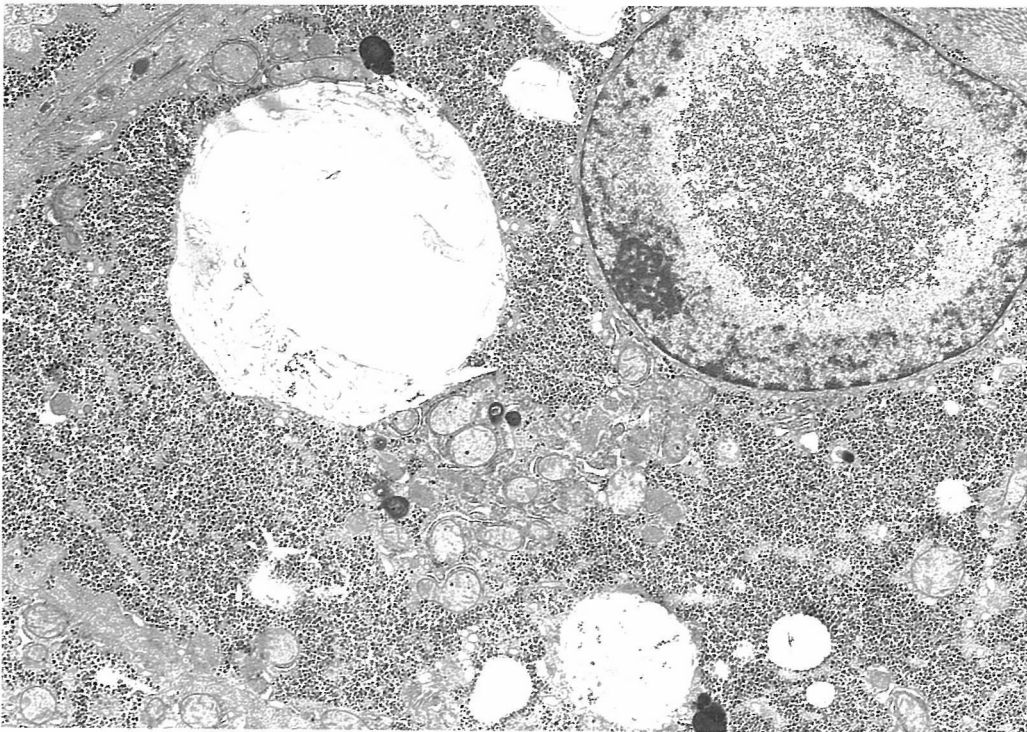


Fig. 3. A large number of glycogen granules are demonstrated in the nucleus and cytoplasm of the hepatocyte from a patient with glycogenosis type III.  $\times 7,000$

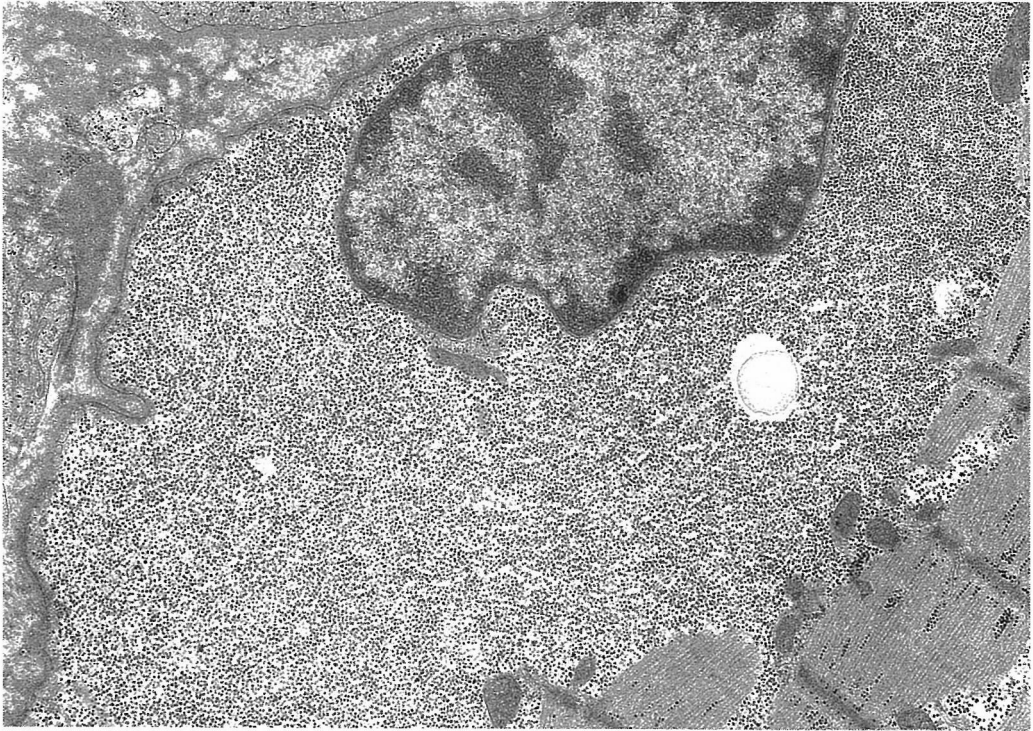


Fig. 4. A large number of glycogen granules are shown in the cytoplasm of the striated muscle cells from same patient in Fig. 3.  $\times 15,000$

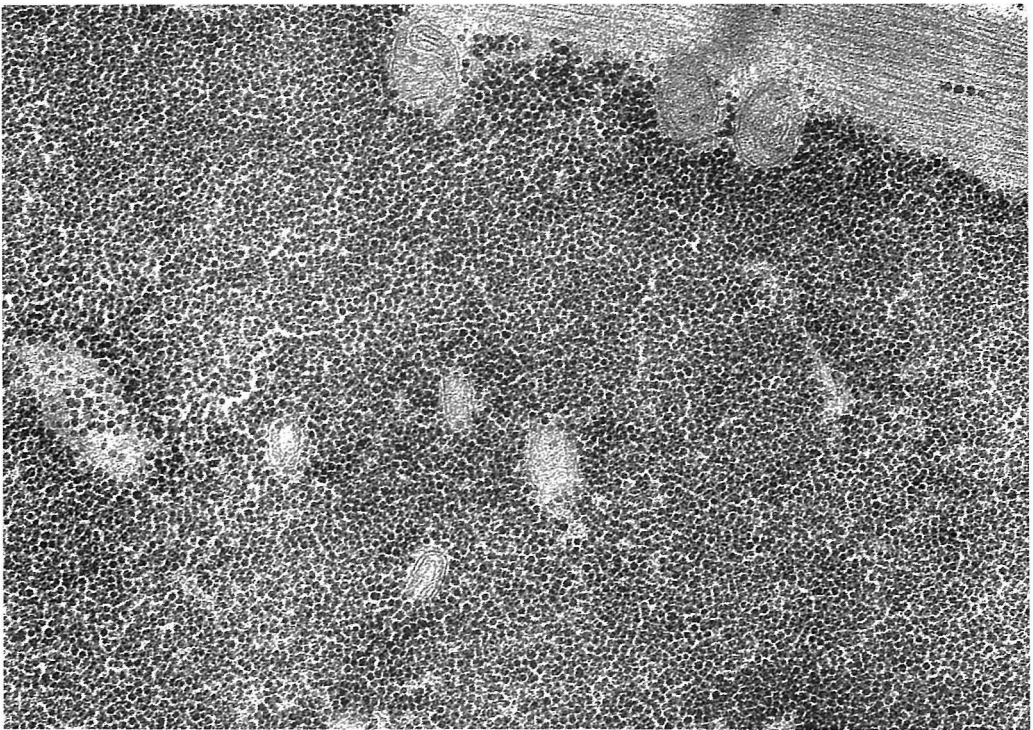


Fig. 5. Glycogen granules are visualized as aggregates of silver particles  
Thiery stain.  $\times 46,000$

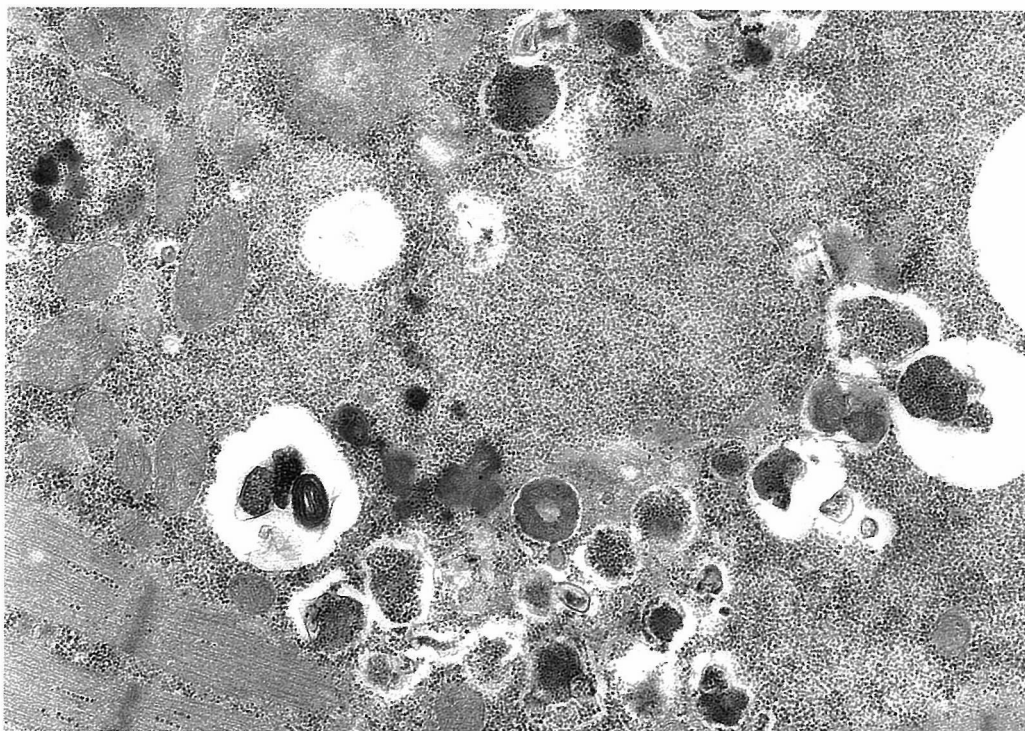


Fig. 6. A large number of glycogen granules and several glycogenosomes are contained in the strained muscle cell from a patient with glycogenosis type II.  $\times 23,000$

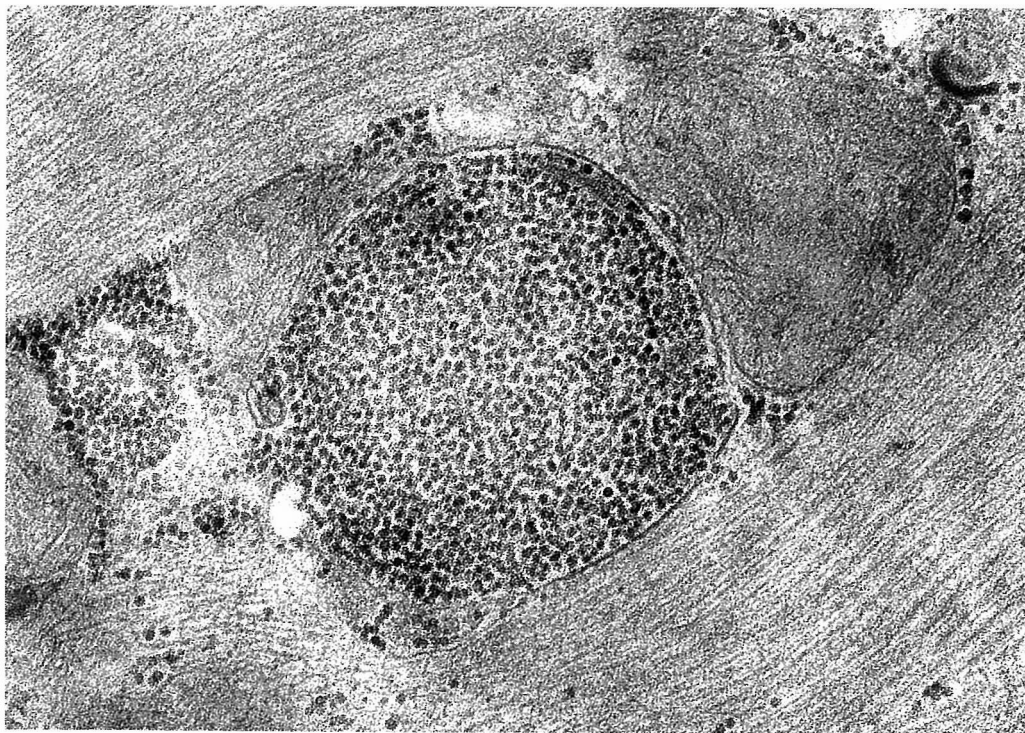


Fig. 7. A glycogenosome containing a large number of glycogen granules is surrounded by a single membrane.  $\times 70,000$



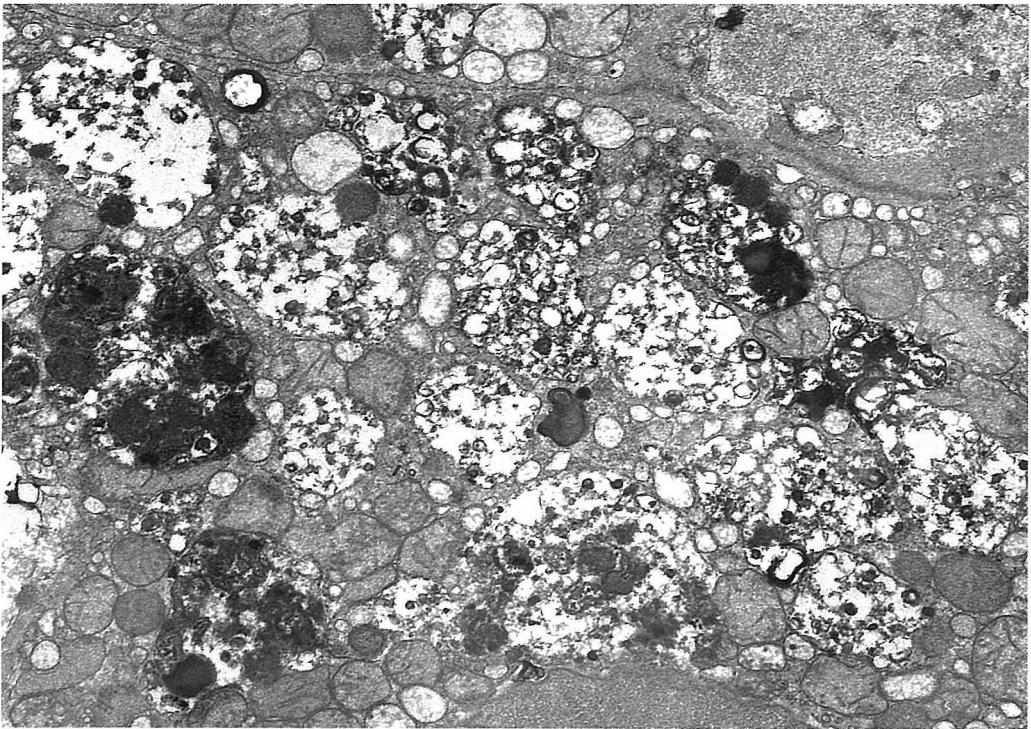


Fig. 8. Many myelin-like materials are demonstrated in the cytoplasm of the hepatocyte from a patient with Niemann-Pick's disease.  $\times 11,000$

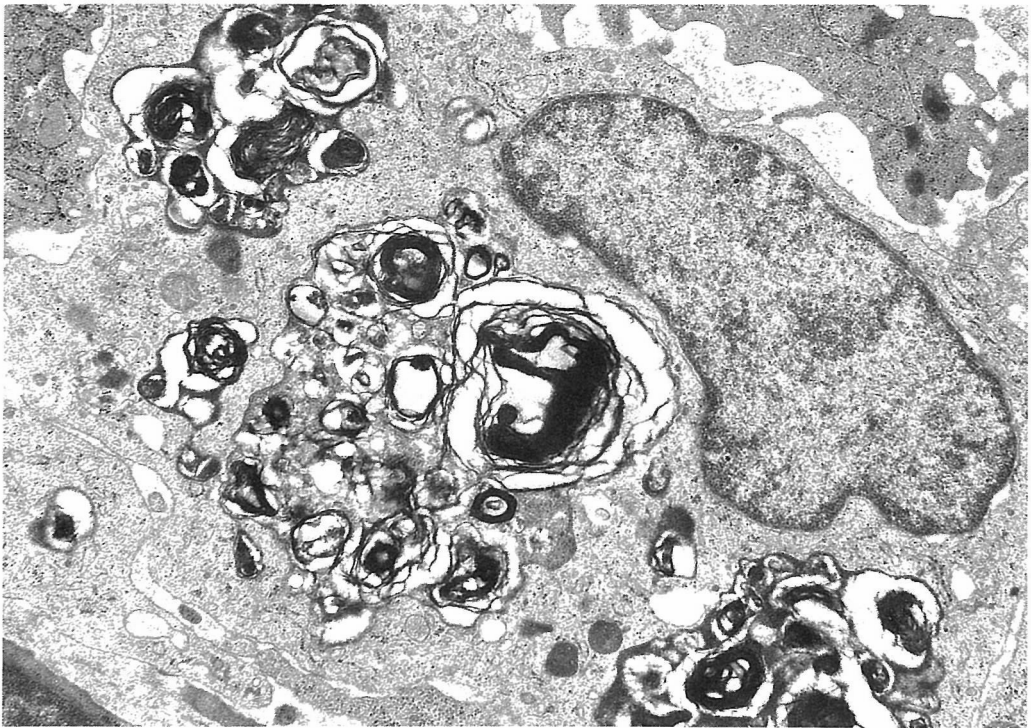


Fig. 9. A large number of myelin-like materials are noted in the splenic macrophage from a patient with idiopathic thrombocytopenic purpura.  $\times 12,000$

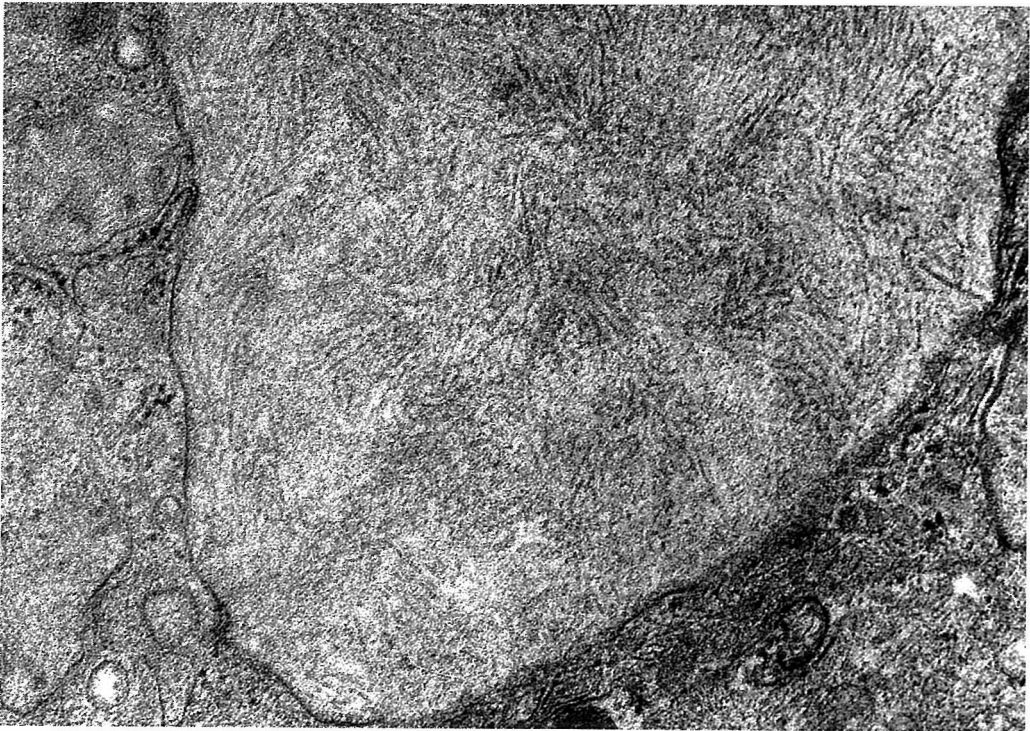


Fig. 10. A large number of tubule-like structures are noted in the cytoplasmic inclusion of splenic macrophage from a patient with hemolytic anemia due to overproduction of adenosine deaminase.  $\times 52,000$

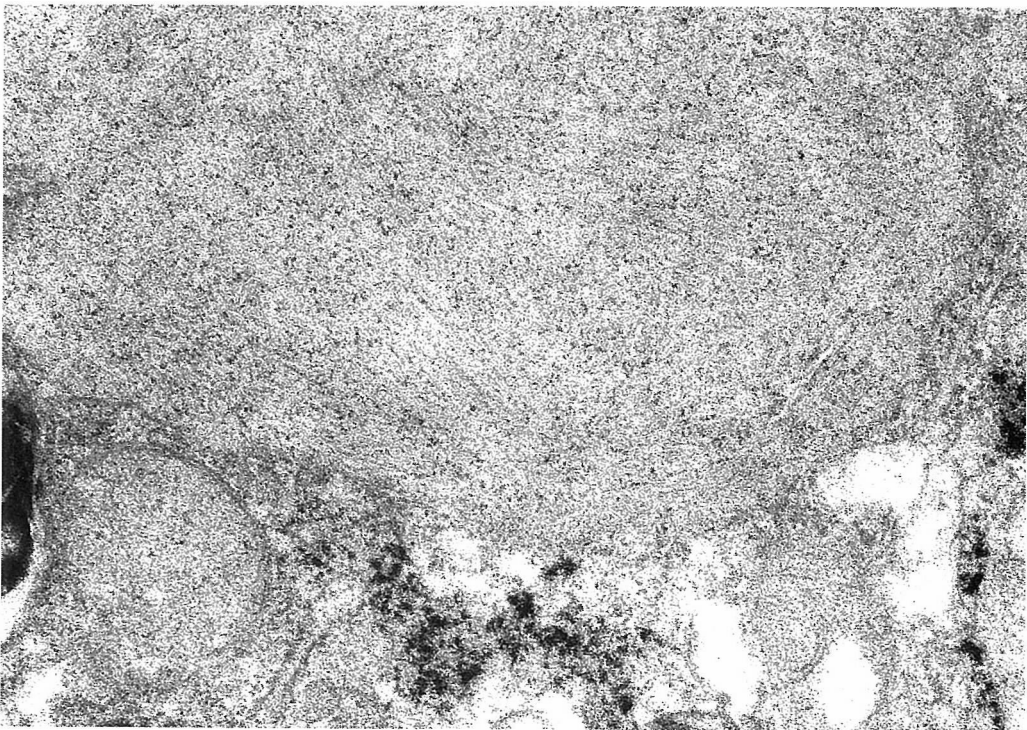


Fig. 11. Acid phosphatase activity is demonstrated in the intracytoplasmic inclusion of the splenic macrophages from same patient in Fig. 10.  $\times 54,000$

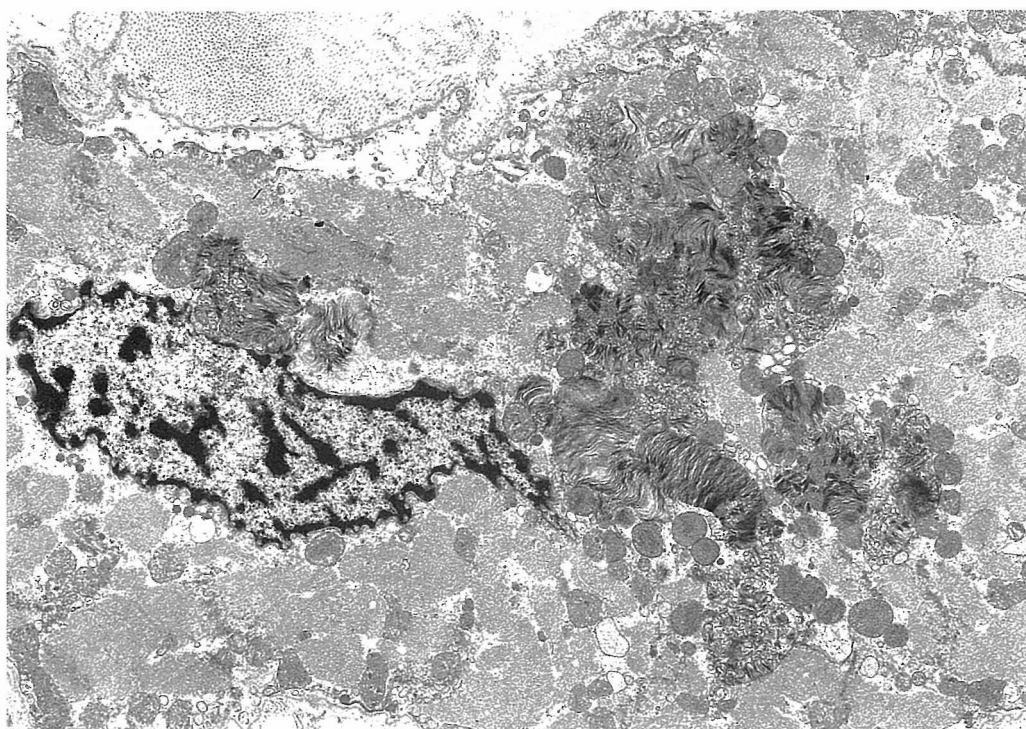


Fig. 12. Various kinds of myelin-like structures are noted in the cytoplasm of the cardiomyocyte from a patient with Fabry's disease.  $\times 7,000$

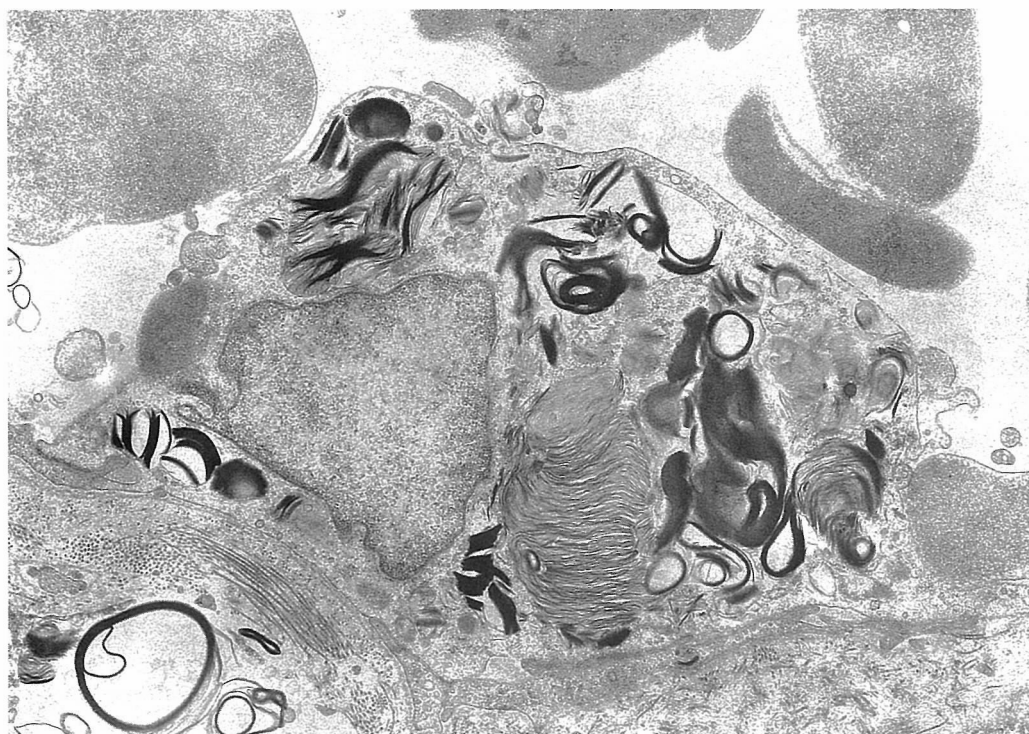


Fig. 13. Myelin-like structures occupy in the cytoplasm of an endothelial cell in the myocardium from the same patient in Fig. 12.  $\times 9,000$



Fig. 14A. The intracytoplasmic inclusion in the cardiomyocyte from the same patient in Figs. 12 and 13 shows rod shaped and finger-print-like structures.  $\times 46,000$

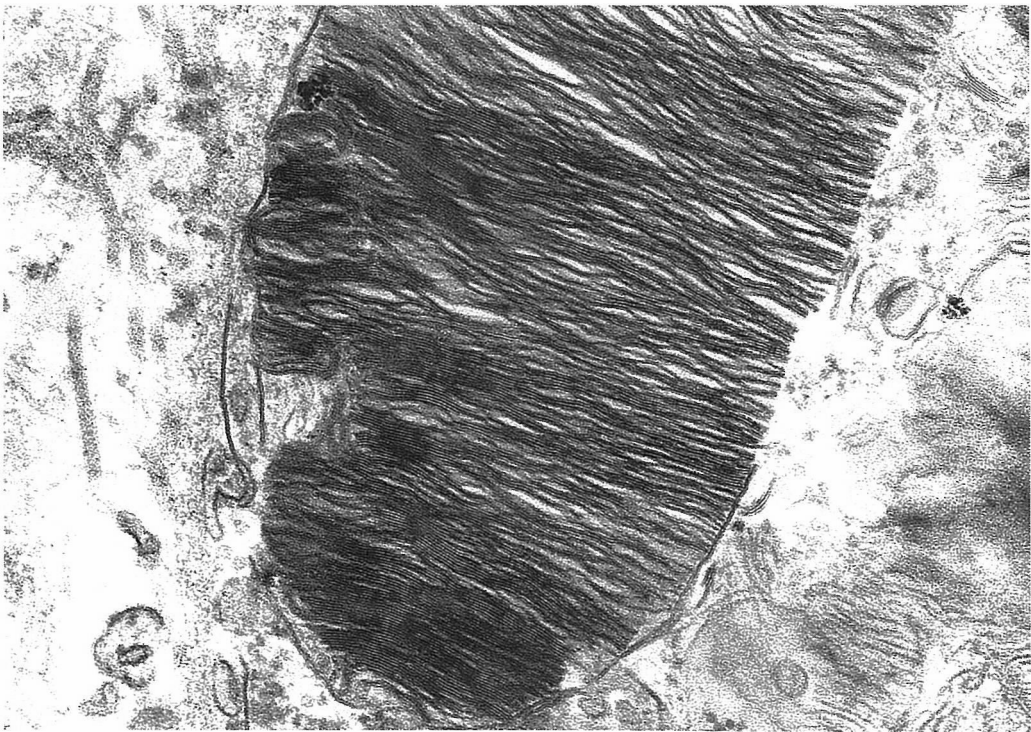


Fig. 14B. The intracytoplasmic inclusion is composed of lamellar myelin-like structures with a periodicity of about 6nm.  $\times 71,000$

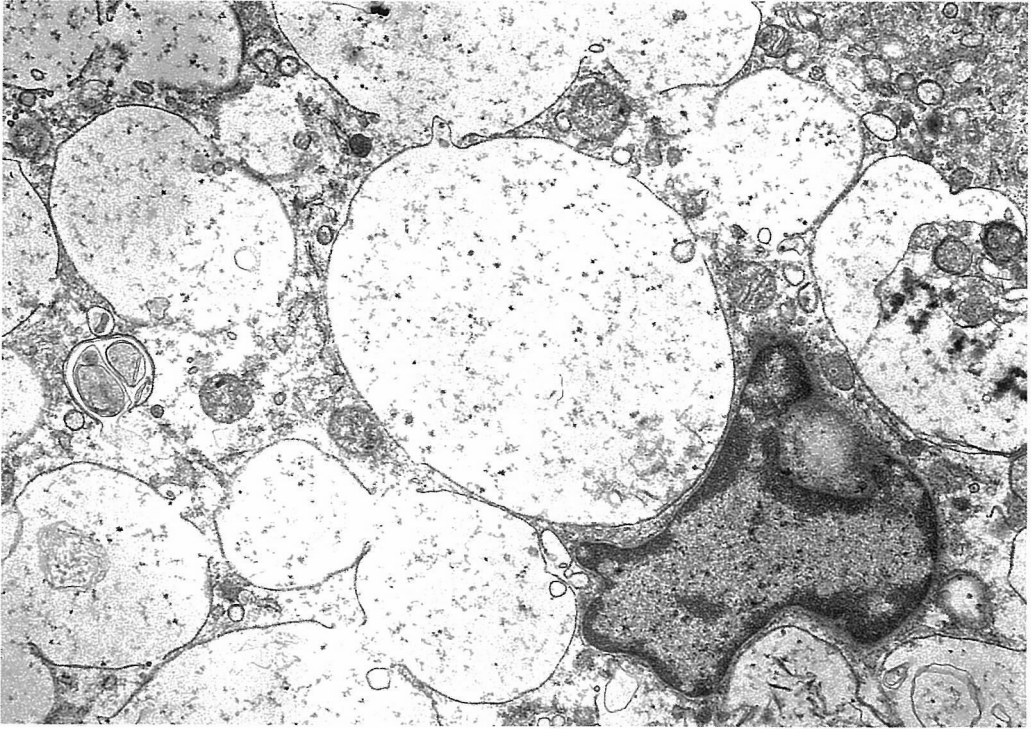


Fig. 15. Intracytoplasmic vacuoles with a few flocculent materials are noted in the hepatocyte from a patient with sialidosis.  $\times 11,000$

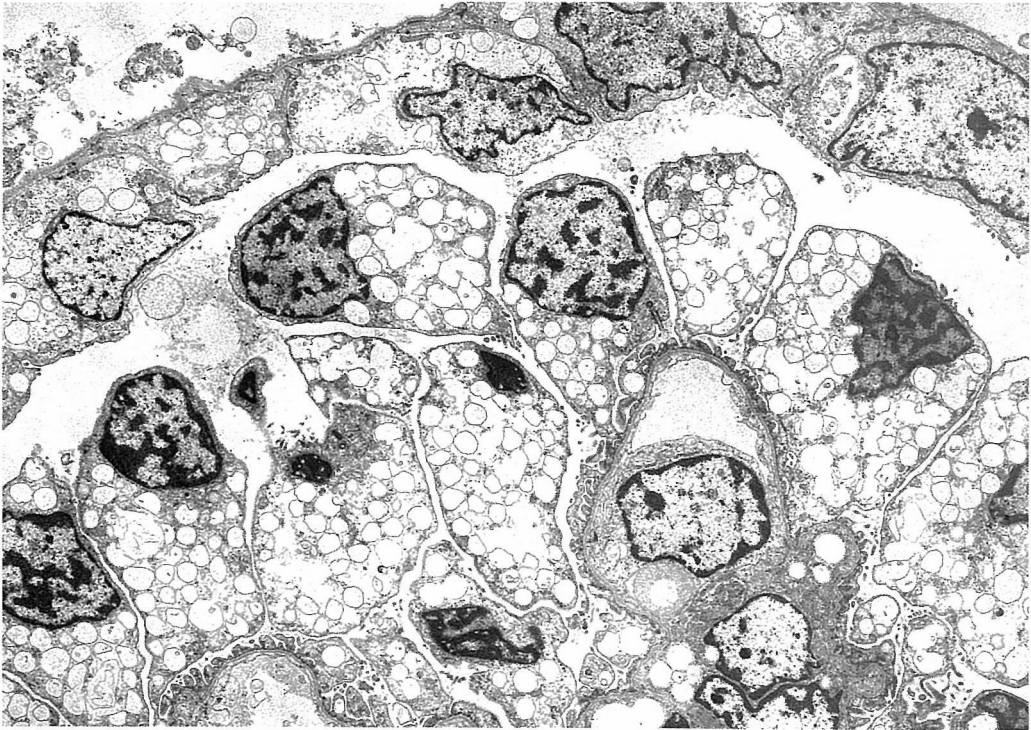


Fig. 16. Many vacuoles are shown in the cytoplasm of epithelial cells of glomerular tuft from a fetus with sialidosis.  $\times 3,000$

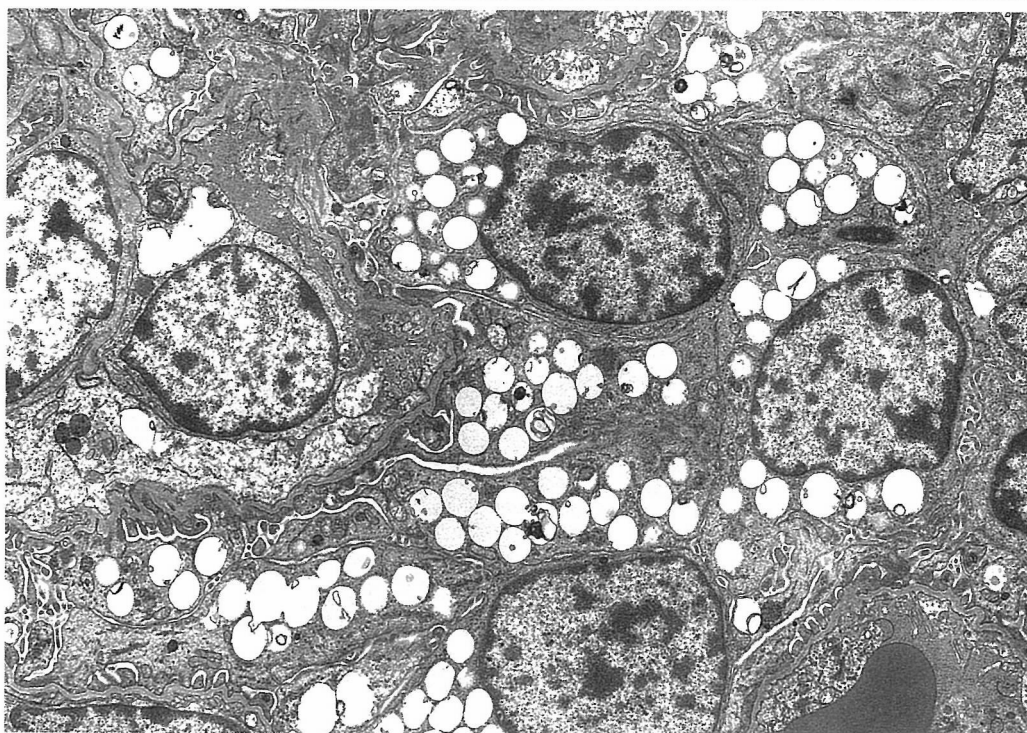


Fig. 18. The intracytoplasmic vacuoles surrounded by a single membrane are contained in the cells of glomerular tuft from a fetus with I-cell disease.  $\times 5,000$

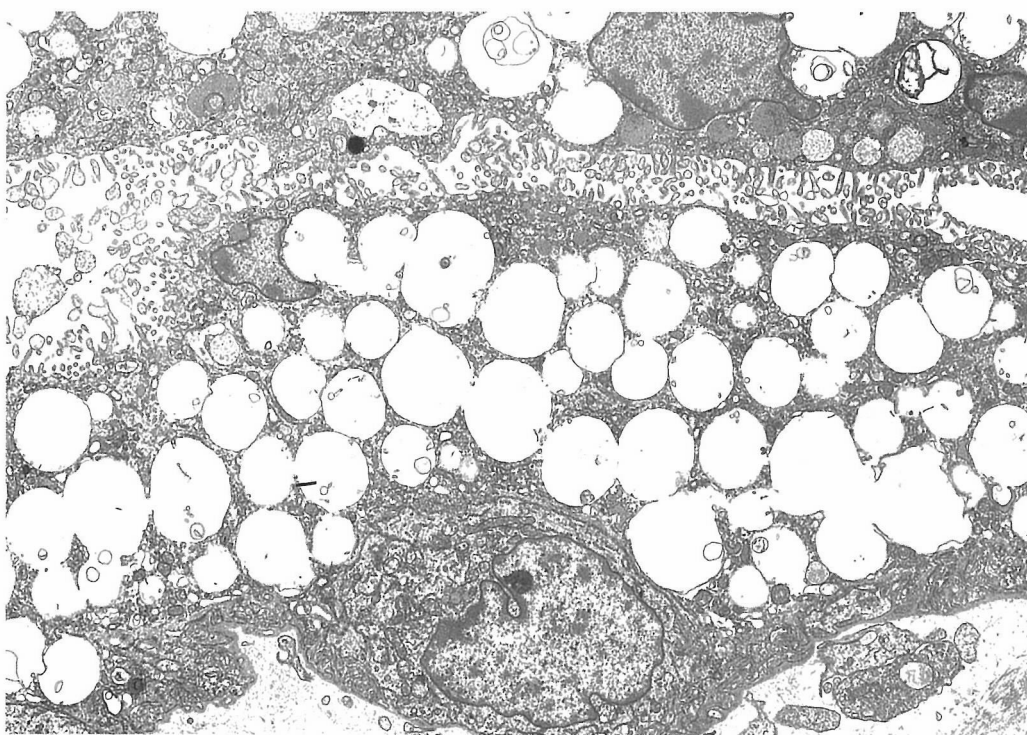


Fig. 19. The inclusion bodies are demonstrated in syncytiotrophoblasts, but not in cytotrophoblasts from the same patient in Fig. 18.  $\times 4,000$

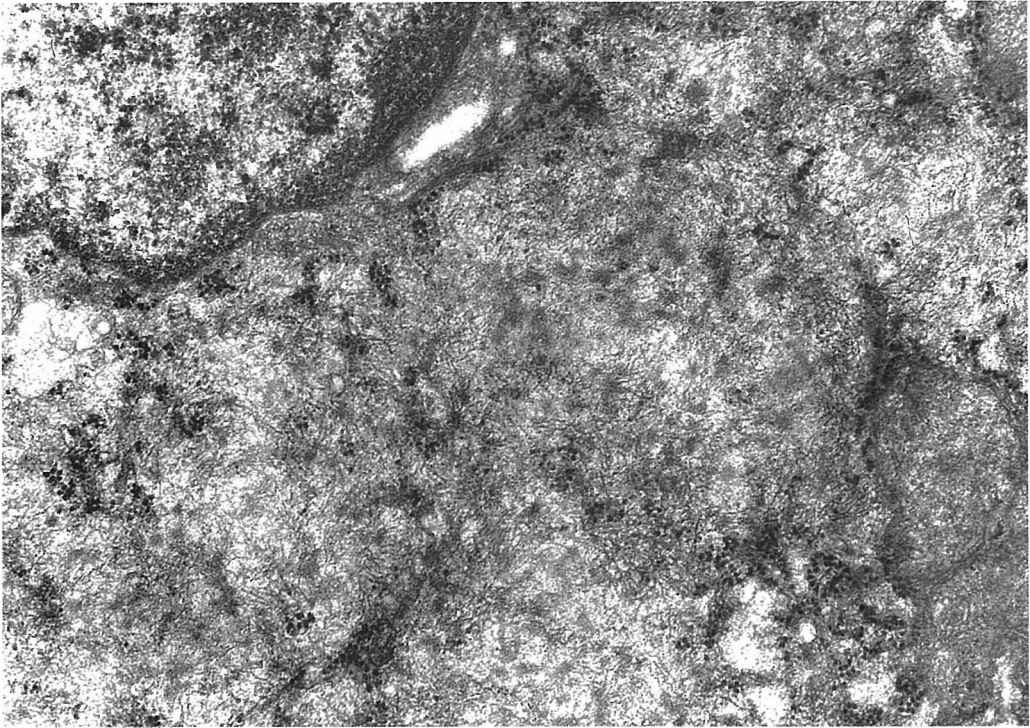


Fig. 21. The intracytoplasmic inclusions composed of membrane-like structures and glycogen granules are noted in the hepatocytes from a patient with glycogenosis type IV.  $\times 30,000$

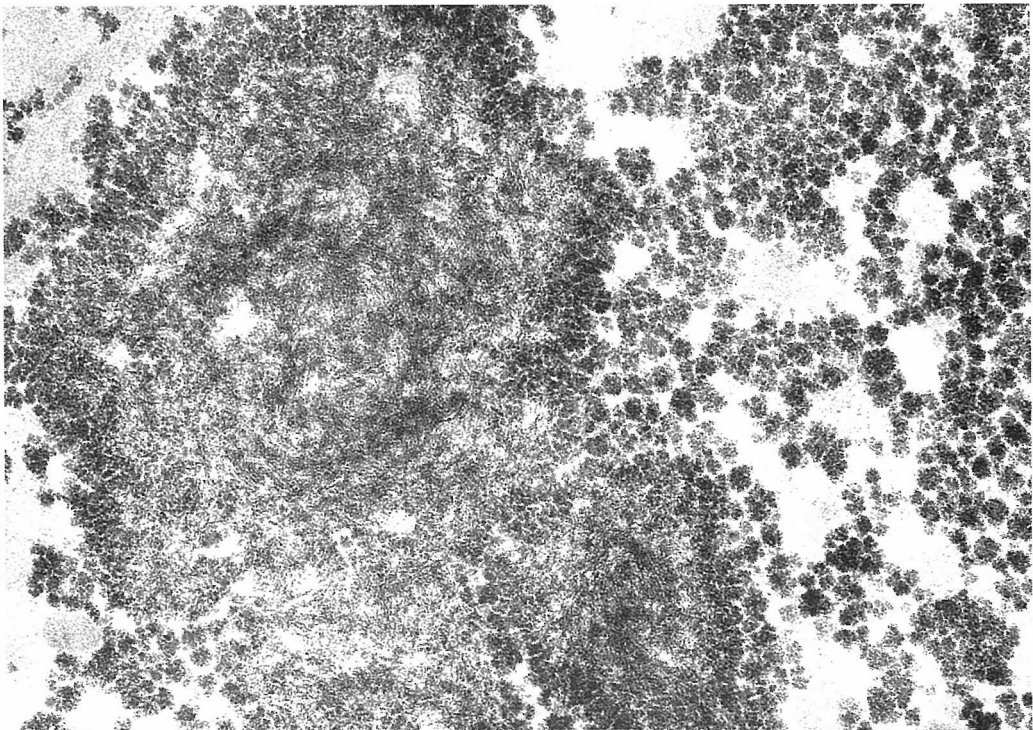


Fig. 22. Glycogen granules and membrane-like structures are visualized as aggregates of silver particles. Thiery stain.  $\times 21,000$

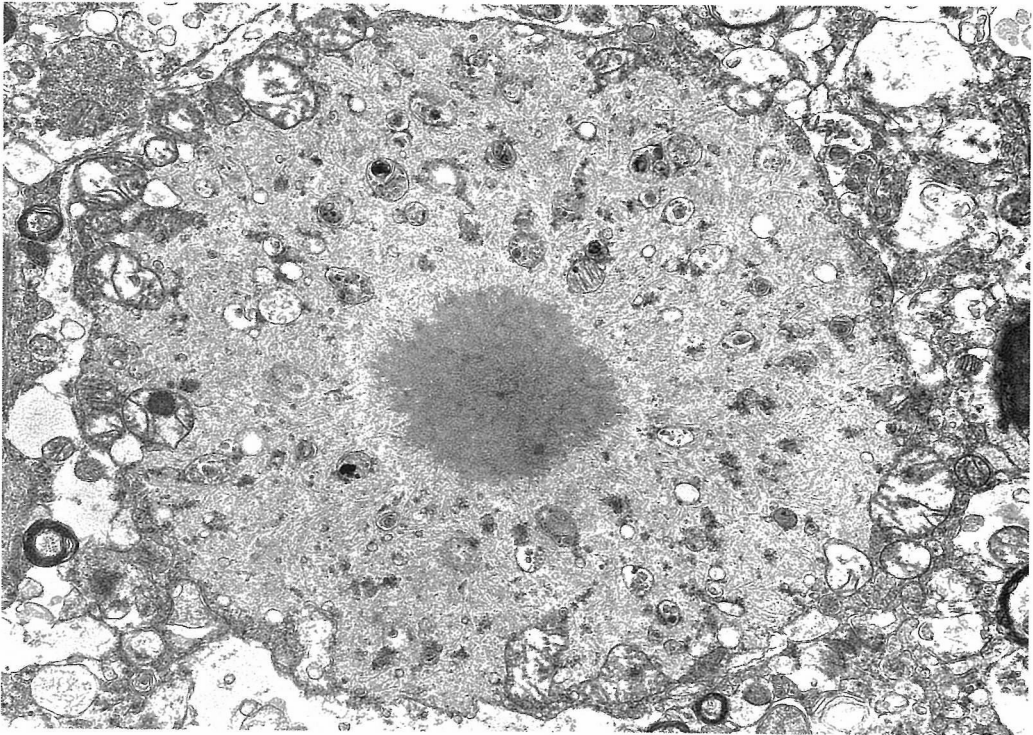


Fig. 25. A Lafora body is composed of membrane-like structures and a few organelle.  $\times 14,000$

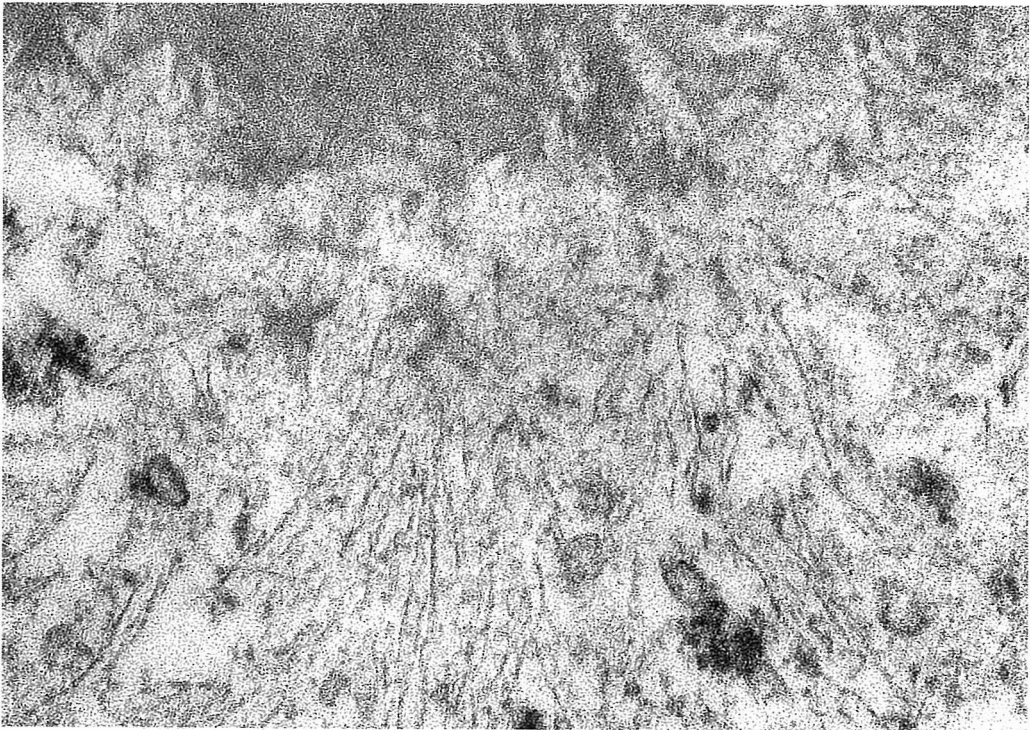


Fig. 26. Dense and homogenous core, and radially oriented membrane-like structures are noted in the Lafora body.  $\times 78,000$



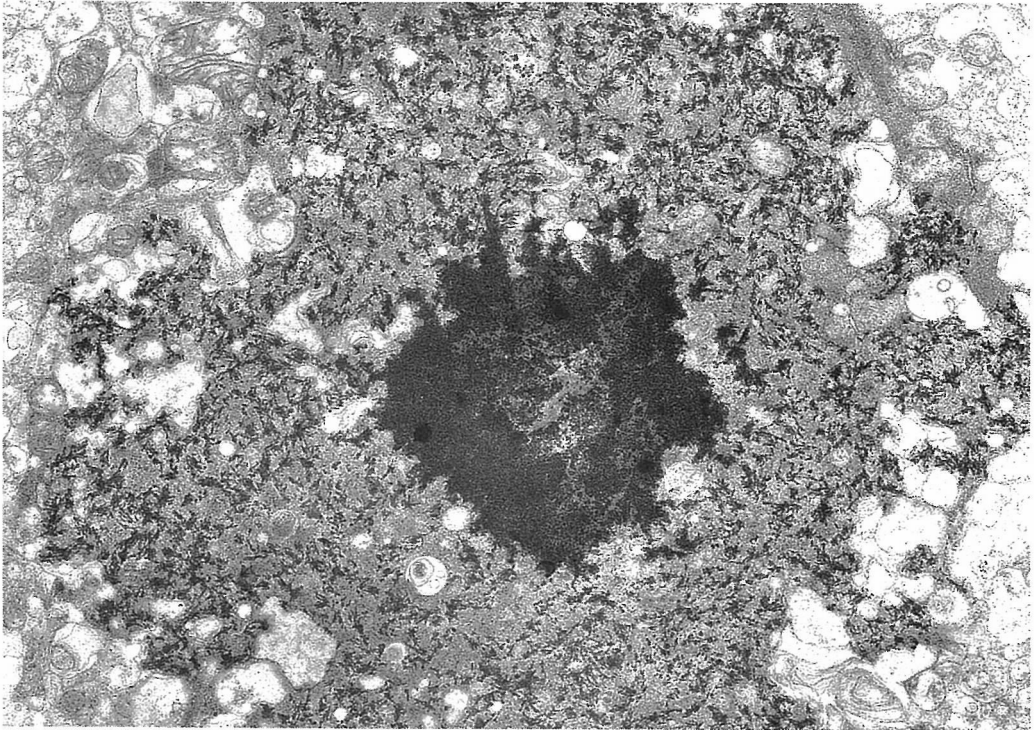


Fig. 27. The membrane-like structures are intensely stained by Thiery staining. Thiery stain.  $\times 9,500$

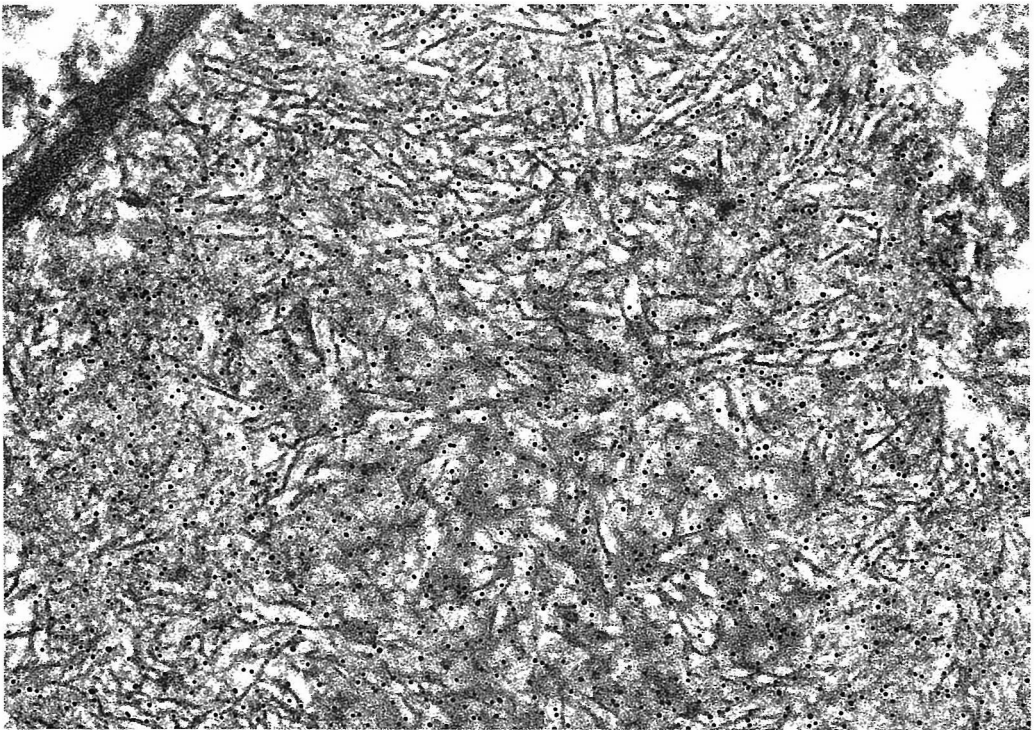


Fig. 28. The membrane-like structures of polyglucosan body in the brain from aged dog are specifically labeled with gold particles indicating reactive to the anti-Lafora body antibody. Immunoelectron microscopy.  $\times 57,000$

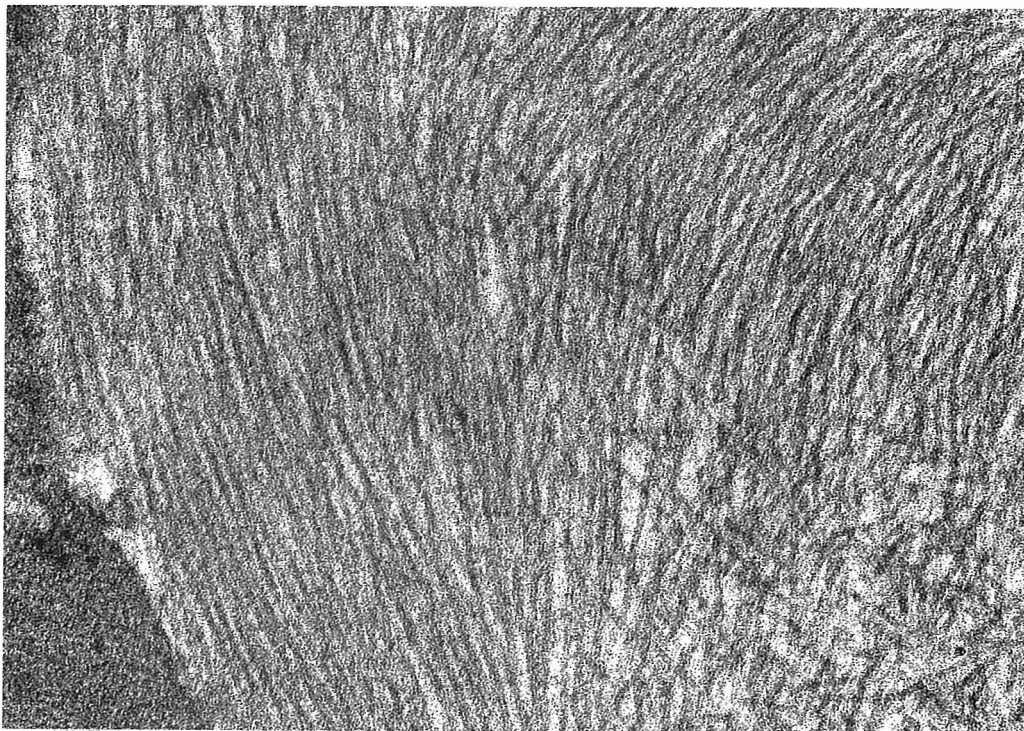


Fig. 30. Amyloid fibrils are nonbranching, fine fibrils, measuring approximately 10 nm in width.  $\times 85,000$

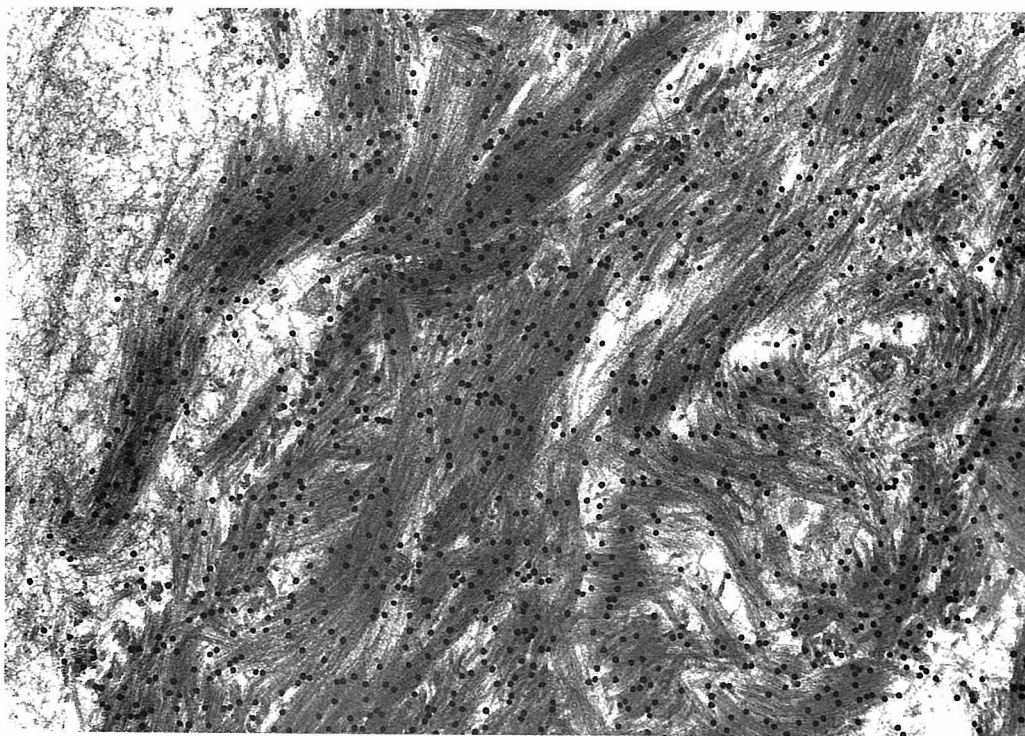


Fig. 31. Amyloid fibrils of hemodialysis associated amyloidosis ( $A\beta_2M$  amyloidosis) are arranged in short curvilinear bundles. The fibrils react to anti- $\beta_2$  microglobulin antiserum. Immunoelectron microscopy.  $\times 53,000$

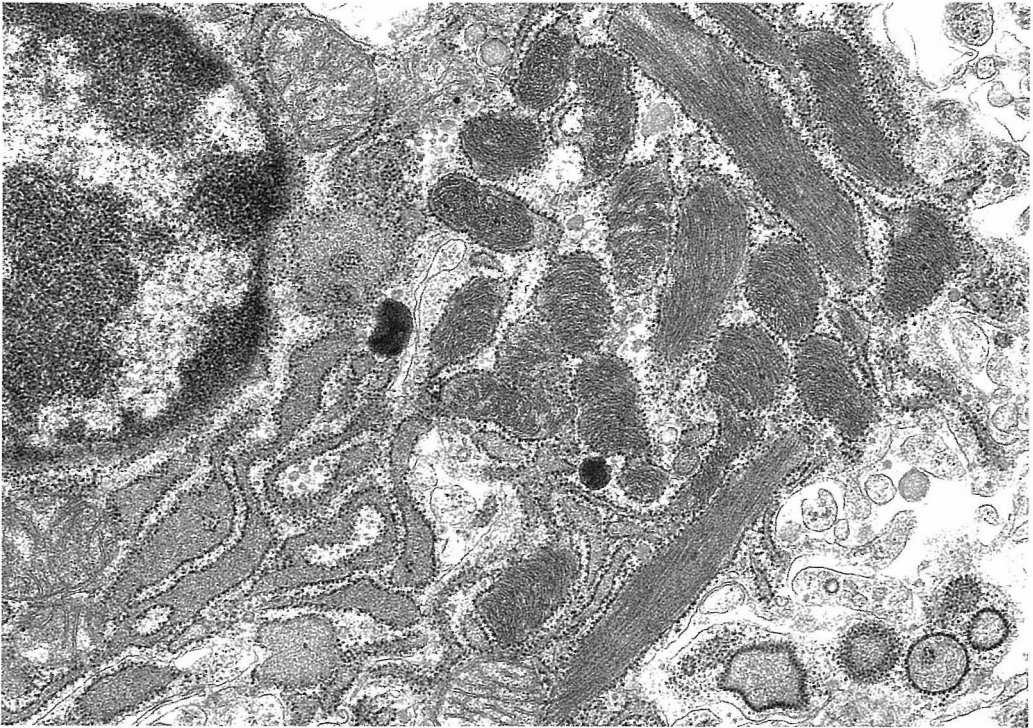


Fig. 32. Fusiform to irregular-shaped inclusions, 0.5 to 1  $\mu\text{m}$  wide and 1 to 5  $\mu\text{m}$  long, are noted in the cytoplasm of the plasma cell from a patient with  $\text{A}\lambda$  localized amyloidosis.  $\times 21,000$

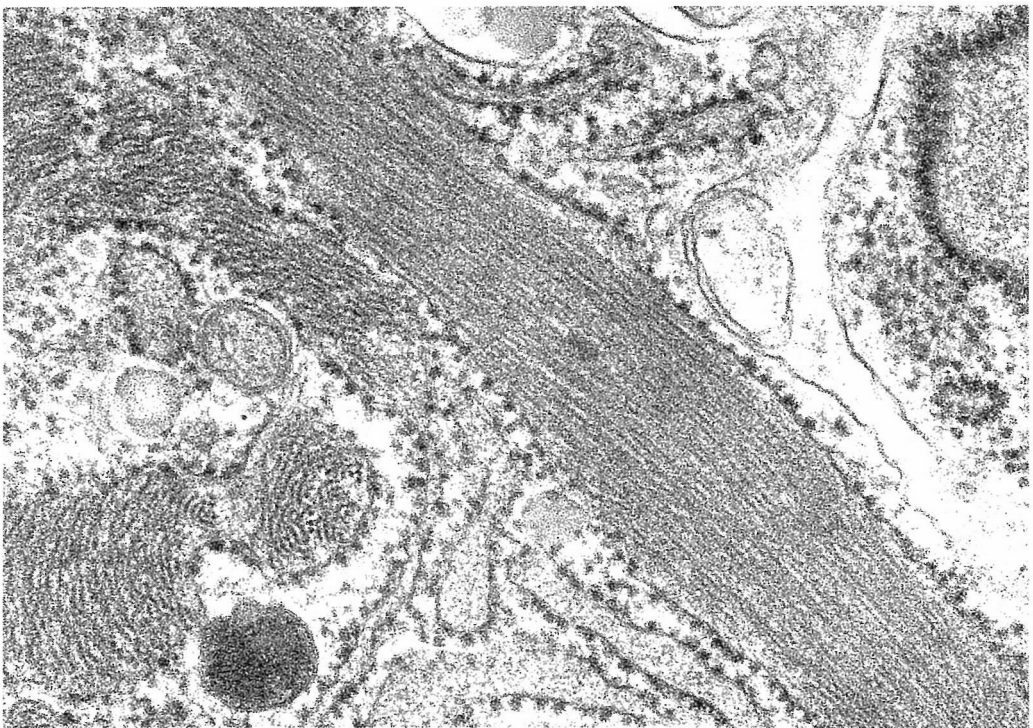


Fig. 33. Regular arrays of fine fibrils are noted in the rough endoplasmic reticulum of the plasma cell from same patient in Fig. 32.  $\times 70,000$

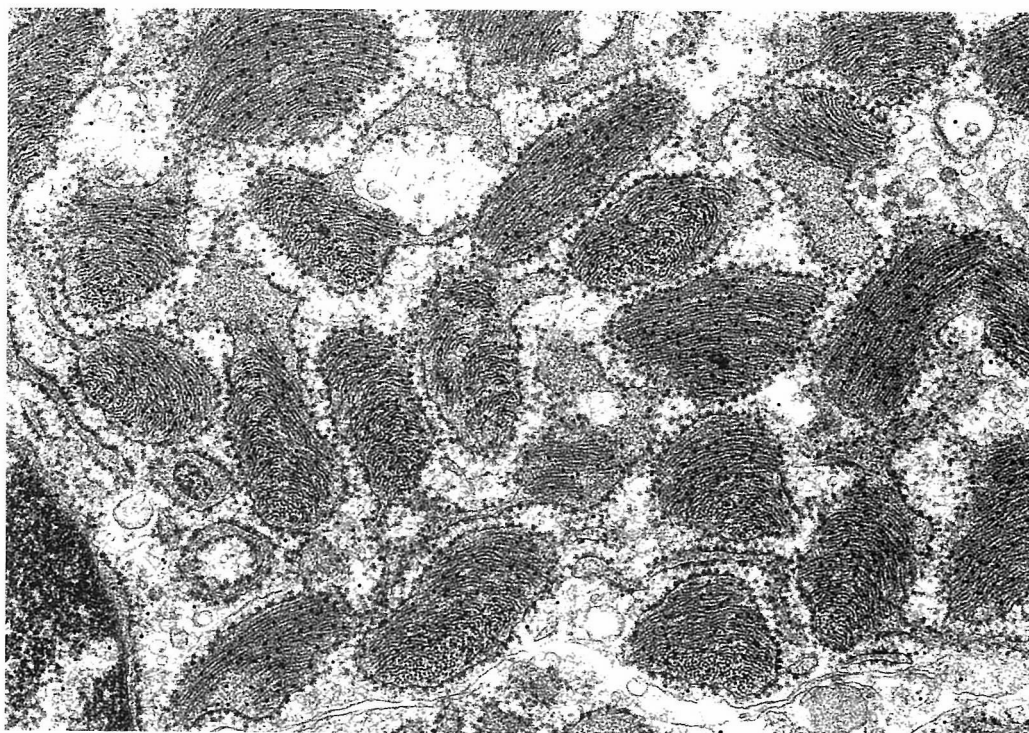


Fig. 34. The fibrils within the rough endoplasmic reticulum of the plasma cell are labeled with gold particles to anti-human A $\lambda$  antiserum. Immunoelectron microscopy.  $\times 35,000$

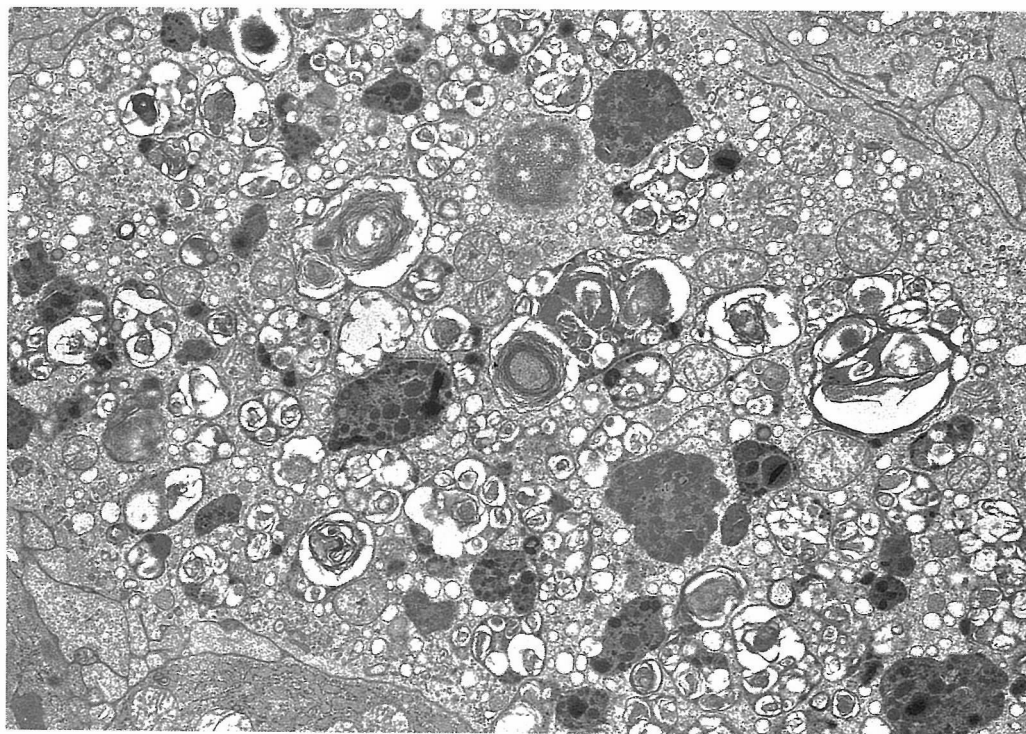


Fig. 35. A large number of myelin-like material and many dense bodies are contained in the macrophage from a patient with Felty syndrome received gold salts.  $\times 7,000$

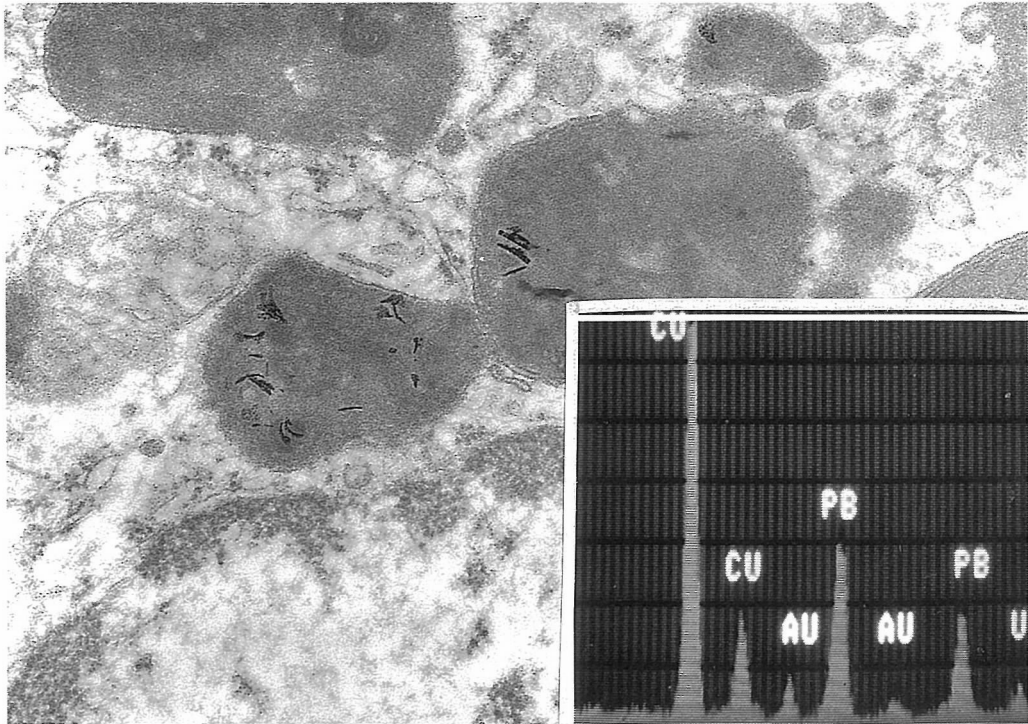


Fig. 36. Several needle-shaped dense bodies are noted in the phagosomes of a macrophage.  
× 37,000 Inset: By x-ray microanalysis, needle-shaped dense bodies contain gold.

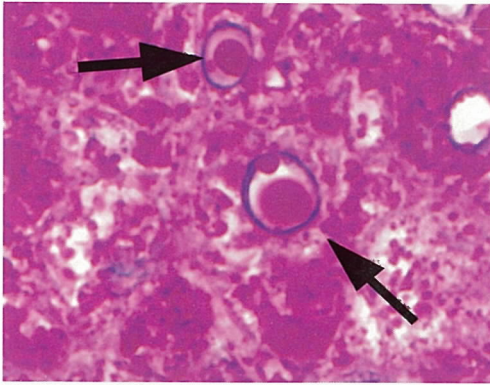


Fig. 2. PAS-positive materials (arrows) are shown in the nuclei of hepatocytes from a patient with glycogenosis type III. PAS stain.

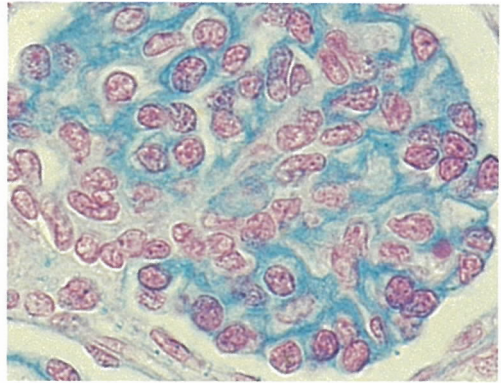


Fig. 17. Inclusions in the epithelial cells of glomerular tuft from a patient with I-cell disease are stained positively with colloidal iron. Colloidal iron stain.

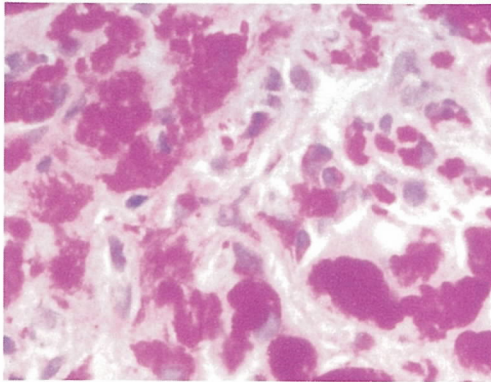


Fig. 20. PAS-positive inclusions showing diastase resistant occupy through the cytoplasm of hepatocytes from a patient with glycogenosis type IV. PAS stain.

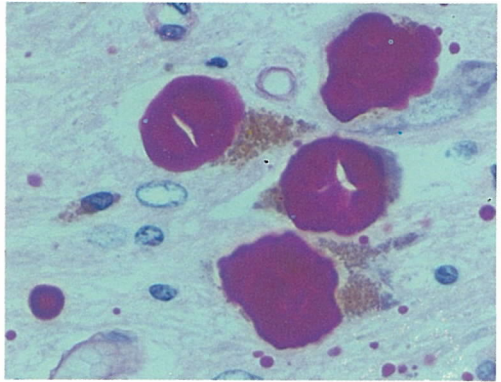


Fig. 23. Large PAS-positive intraneural inclusions known as Lafora body are demonstrated in the brain from a patient with Lafora's disease. PAS stain.

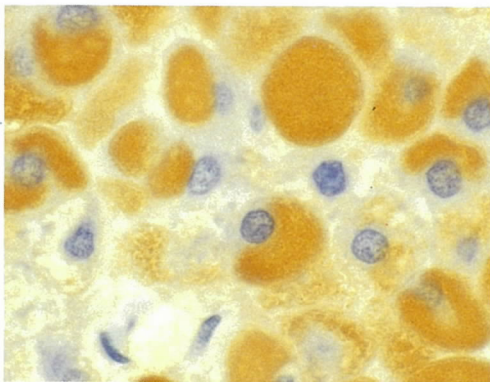


Fig. 24. Intracytoplasmic inclusions in the hepatocytes from a patient with Lafora's disease are strongly reactive with anti-Lafora body antibody.



Fig. 29. Congo red positive materials show birefringence and dichroism under polarized light.